

# Indian Ocean Dipole: Processes and impacts

P N VINAYACHANDRAN<sup>1,\*</sup>, P A FRANCIS<sup>2</sup> and S A RAO<sup>3</sup>

<sup>1</sup>*Centre for Atmospheric and Oceanic Sciences, Indian Institute of Science, Bangalore 560 012, India*

<sup>2</sup>*Indian National Centre for Ocean Information Services, Hyderabad 500 055, India*

<sup>3</sup>*Indian Institute of Tropical Meteorology, Pashan, Pune 411 008, India*

\* e-mail: vinay@caos.iisc.ernet.in

Equatorial Indian Ocean is warmer in the east, has a deeper thermocline and mixed layer, and supports a more convective atmosphere than in the west. During certain years, the eastern Indian Ocean becomes unusually cold, anomalous winds blow from east to west along the equator and southeastward off the coast of Sumatra, thermocline and mixed layer lift up and the atmospheric convection gets suppressed. At the same time, western Indian Ocean becomes warmer and enhances atmospheric convection. This coupled ocean-atmospheric phenomenon in which convection, winds, sea surface temperature (SST) and thermocline take part actively is known as the Indian Ocean Dipole (IOD). Propagation of baroclinic Kelvin and Rossby waves excited by anomalous winds, play an important role in the development of SST anomalies associated with the IOD. Since mean thermocline in the Indian Ocean is deep compared to the Pacific, it was believed for a long time that the Indian Ocean is passive and merely responds to the atmospheric forcing. Discovery of the IOD and studies that followed demonstrate that the Indian Ocean can sustain its own intrinsic coupled ocean-atmosphere processes. About 50% percent of the IOD events in the past 100 years have co-occurred with El Niño Southern Oscillation (ENSO) and the other half independently. Coupled models have been able to reproduce IOD events and process experiments by such models – switching ENSO on and off – support the hypothesis based on observations that IOD events develop either in the presence or absence of ENSO. There is a general consensus among different coupled models as well as analysis of data that IOD events co-occurring during the ENSO are forced by a zonal shift in the descending branch of Walker cell over to the eastern Indian Ocean. Processes that initiate the IOD in the absence of ENSO are not clear, although several studies suggest that anomalies of Hadley circulation are the most probable forcing function. Impact of the IOD is felt in the vicinity of Indian Ocean as well as in remote regions. During IOD events, biological productivity of the eastern Indian Ocean increases and this in turn leads to death of corals over a large area. Moreover, the IOD affects rainfall over the maritime continent, Indian subcontinent, Australia and eastern Africa. The maritime continent and Australia suffer from deficit rainfall whereas India and east Africa receive excess. Despite the successful hindcast of the 2006 IOD by a coupled model, forecasting IOD events and their implications to rainfall variability remains a major challenge as understanding reasons behind an increase in frequency of IOD events in recent decades.

## 1. Introduction

Monsoons dominate the climate of the North Indian Ocean and the neighbouring land mass. Winds over the Indian Ocean (figure 1) blow from

the southwest during May–September and north-east during November–February and drive a circulation that reverses its direction completely, unseen in any other part of the world oceans (Schott and McCreary 2001; Shankar *et al* 2002). Because

**Keywords.** Indian Ocean Dipole; oceanography; interannual variability.

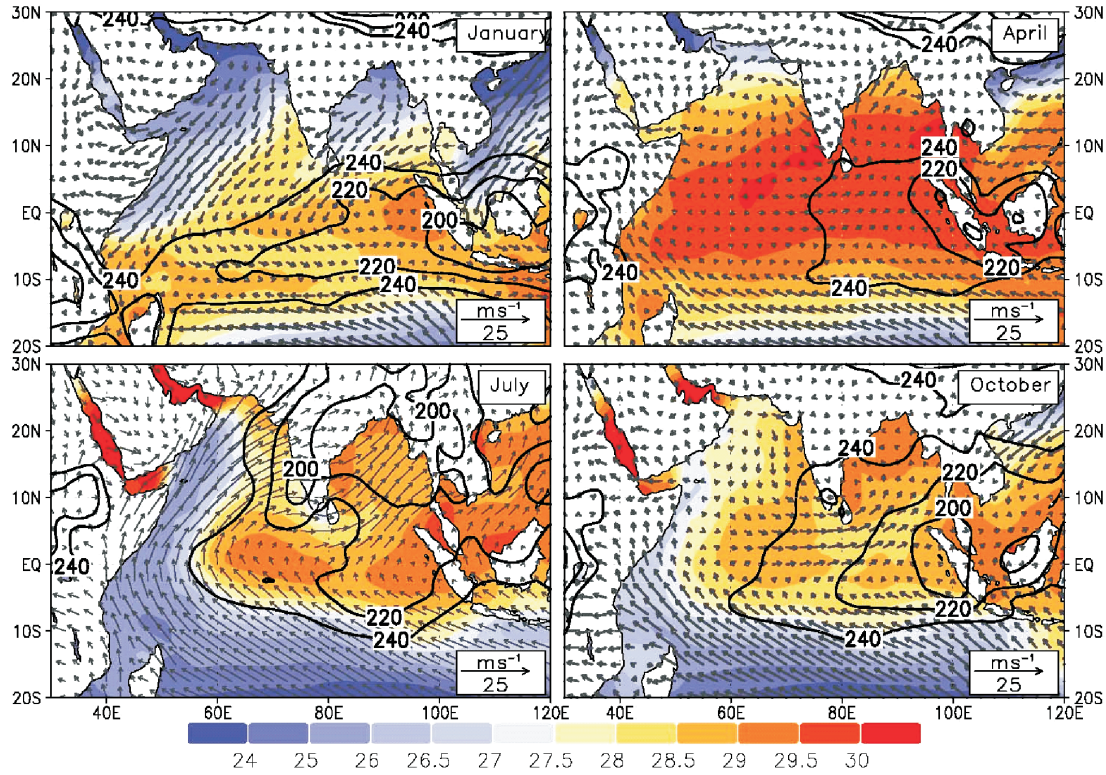


**Figure 1.** Climatology of winds (vectors in m/s), SST ( $^{\circ}$ C, color shaded) and outgoing longwave radiation (OLR, contours in  $\text{Wm}^{-2}$ ) over the Indian Ocean.

of monsoons, the spatial distribution of sea surface temperature (SST) in the Indian Ocean is characterised by warm water on the eastern side and cooler on the west which is in contrast to Pacific and Atlantic Oceans that are warmer on the west. In fact, all characteristic properties of the ocean show marked east-west asymmetry in Indian Ocean. Freshwater input into the ocean, in the form of rain and drainage from the land, is greater on eastern side causing the eastern part of the basin to have lower salinity than the west. A major upwelling system is located off the western boundary and consequently biological productivity is higher in the west than in the east. The thermocline, which separates warmer water of the oceanic mixed layer from the colder water underneath, is located deeper in the east than in the west. Asymmetry in the SST also influences the overlying atmosphere: convection is higher over the eastern part of the ocean and lesser over the west (figure 1).

The equatorial Indian Ocean, however, experiences a somewhat different seasonal wind forcing and hence has a different response than the Arabian Sea and Bay of Bengal. Winds over the equatorial Indian Ocean, particularly their zonal component, are weak during monsoons. Relatively strong westerly winds, however, appear during the transition between monsoons, first during

April-May (spring) and then again during October-November (fall). These winds drive strong eastward currents along the equator, attaining speeds exceeding  $1 \text{ ms}^{-1}$ , known as Wyrtki (1973) jets. Wyrtki jets transport warmer upper layer water towards the east, which accumulates near the boundary causing the thermocline in the east to be deeper than in the west. The thermocline slope becomes greater during spring and fall and the volume of warm water and the heat content of the Indian Ocean is larger on the eastern side than in the west. When the thermocline is shallow, winds have to do lesser work to bring cooler water into the mixed layer than when it is deep. That is, for the same wind-strength, a shallower thermocline can facilitate cooling of the mixed layer and SST, whereas a deeper thermocline may not. Thus, Wyrtki jets dictate the shape of the thermocline in the equatorial Indian Ocean. Climatologically, since the eastern equatorial Indian Ocean is warmer, it supports a more convective atmosphere than in the west (figure 1). The departure of the ocean-atmosphere system from this mean state occurring during certain years, characterized by opposite sign of anomalies in the east and west, is known as the Indian Ocean Dipole (IOD).

Possibilities of air-sea coupled processes over the Indian Ocean have been suggested by several studies in the past. Reverdin *et al* (1986) analyzed

interannual variations of convection and SST in the equatorial Indian Ocean using ship reports. They suggested that coupled air-sea dynamics over the Indian Ocean should be considered in order to understand the interannual variability. This suggestion was prompted by anomalous conditions in 1961, characterized by significantly cold SST anomalies in the east (between 80°E–90°E) and warm SST anomalies (SSTA) in the west. From limited ship observations, Reverdin *et al* (1986) concluded that the SSTA affects cloudiness, rainfall and consequently, causes westward wind anomalies along the equator. Anomalies during 1961 were not concurrent with an ENSO which pointed to the role of air-sea interaction processes controlled by Indian Ocean. Hastenrath *et al* (1993) showed that zonal structure of the equatorial Indian Ocean responds to changes in the strength of westerlies occurring during the transition from summer to winter monsoon (October–November). Stronger westerlies drive a faster equatorial jet causing deeper mixed layer and warmer SSTs in the east and entails cold water upwelling in the western equatorial Indian Ocean. Changes in the ocean state affect the atmosphere, particularly rainfall over eastern Africa. SST variability in the eastern Indian Ocean during 1994 was observed to have strong coupling to the shallowing of the thermocline (Meyers 1996). The shallow thermocline during 1994 was due to unusually weak equatorial jets (Vinayachandran *et al* 1999) caused by anomalous easterly winds. Saji *et al* (1999) recognised anomalous conditions such as in 1961, 1994 and 1997 in the tropical Indian Ocean as a dipole mode characterized by low SST off Sumatra and high SST in the western equatorial Indian Ocean accompanied by wind and rainfall anomalies. They showed that the IOD is a coupled ocean atmosphere phenomenon, it is independent of ENSO and about 12% of the SST variability in the Indian Ocean was associated with the dipole mode. Highlighting the 1997–98 event Webster *et al* (1999) also have suggested that anomalous conditions present during this period was due to an internal mode of the climate system of the Indian Ocean. A coupled ocean atmosphere process in which oceanic Rossby waves cause a deepening of the thermocline was proposed to be a necessary feature that led to the sequence of events culminating in anomalies that contrast the in east-west direction (Webster *et al* 1999). The ocean-atmosphere coupling during an IOD involves atmospheric convection, winds, SST and upper ocean dynamics. The discovery of the IOD led to the recognition that the Indian Ocean can support its own coupled ocean-atmosphere variations (Schott *et al* 2009) and is not merely a slave to the events happening over the Pacific Ocean in connection with ENSO.

The Indian Ocean circulation and its impact on regional climate has been a topic of great interest recently and several reviews have appeared in the literature. The monsoon circulation of the Indian Ocean has been reviewed by Schott and McCreary (2001). Yamagata *et al* (2004) and Annamalai and Murtugudde (2004) have reviewed the interannual variability in the Indian Ocean and its impact on climate variability. The role of tropical Atlantic, Pacific and Indian Oceans on climate variability in the tropics has been reviewed by Chang *et al* (2006). In a recent review, Schott *et al* (2009) have summarized the role of Indian Ocean circulation on climate variability. It is well recognised that the dominant signal of coupled interannual variability in the Indian Ocean is the IOD. The objective of this review is to summarize our understanding of the IOD, particularly the processes associated with IOD events and their implications, considering that there has been rapid development in our understanding of these. A description of the IOD phenomenon is given in the next section followed by a section devoted to processes related to IOD. The relationship between ENSO and IOD is discussed in section 4, followed by mechanisms that can trigger IOD in section 5. Section 6 summarizes the impact of IOD on regional climate and outstanding issues are listed in section 7.

## 2. Indian ocean dipole

The Indian Ocean Dipole refers to an anomalous state of the ocean-atmosphere system (Saji *et al* 1999; Webster *et al* 1999; Murtugudde *et al* 2000). During the mature phase of an IOD, which happens during September–October, eastern equatorial Indian Ocean becomes unusually cold and the western equatorial Indian Ocean unusually warm (figure 2). Cold SSTA suppress atmospheric convection in the east whereas warm SSTA enhance convection in the west. Winds blow westward over the equatorial Indian Ocean and from the southwest off the coast of Sumatra, the latter being favourable for coastal upwelling. Equatorial jets become weak, reducing the eastward transport of warm water entailing a shallower than usual thermocline in the east. Sea level decreases in the eastern equatorial Indian Ocean and rises in the central part. Thermocline rises in the east and deepens in the central and western equatorial Indian Ocean. Temperature anomalies associated with IOD are also seen in subsurface ocean (Vinayachandran *et al* 2002; Horii *et al* 2008) and the sub-surface signals are strongly coupled to surface signals (Rao *et al* 2002). Due to the vertical movement of isotherms, magnitude of temperature anomalies at any given depth

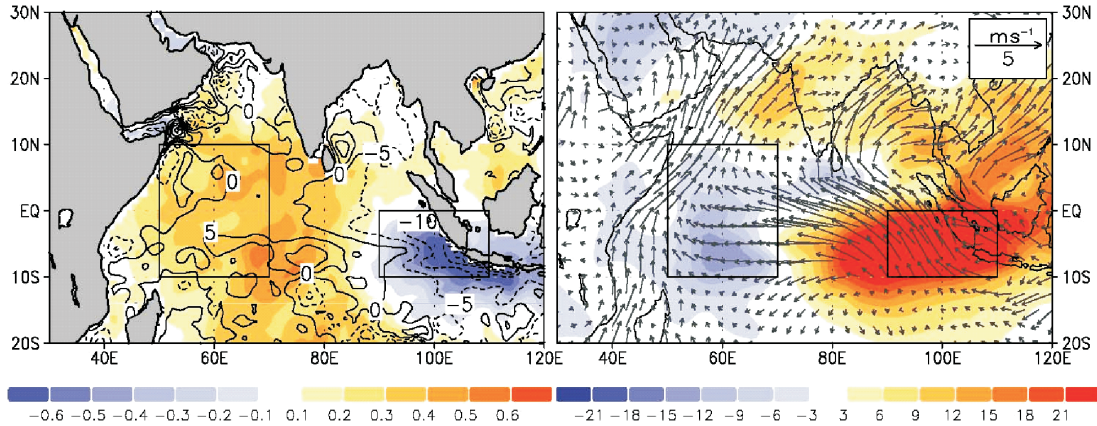


**Figure 2.** Mean September–October composite anomaly patterns of (a) SST ( $^{\circ}\text{C}$ , shaded) and depth of  $20^{\circ}\text{C}$  isotherm (m, contours) and (b) OLR ( $\text{W m}^{-2}$ , shaded) and surface winds ( $\text{ms}^{-1}$ , vectors) for the positive IOD years during 1979–2008 for which satellite data of OLR is available. The composite is based on positive IOD years (Meyers *et al* 2007) of 1982, 1991, 1994, 1997 and 2006. SST data used is HadISST available at (<http://badc.nerc.ac.uk>); depth of  $20^{\circ}\text{C}$  isotherm is derived from simple ocean data assimilation (SODA, Carton *et al* 2000) available at (<http://iridl.ldeo.columbia.edu>); NOAA AVHRR OLR data and NCEP Reanalysis surface wind data are obtained from (<http://www.cdc.noaa.gov>).

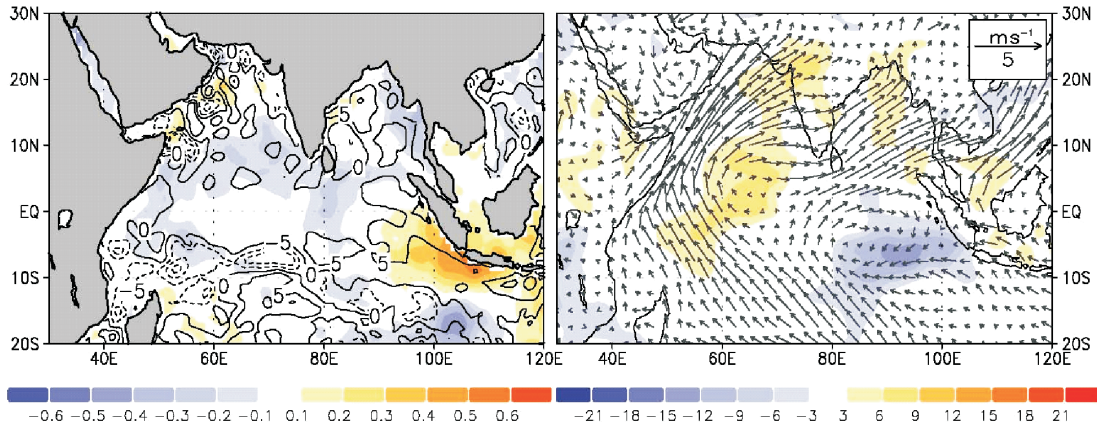


**Figure 3.** Same as in figure 2, but for negative IOD years since 1979 listed in Meyers *et al* (2007), i.e. 1980, 1981, 1985 and 1992.

is much greater than at the surface. Anomalous state of the ocean-atmosphere system described above is referred to as a positive IOD (pIOD). The reverse, negative IOD (nIOD), also occurs, characterized by warmer SSTA, enhanced convection, higher sea level, deeper thermocline in the east and cooler SSTA, lower sea level, shallower thermocline and suppressed convection in the west (figure 3). Negative IOD can be considered as an intensification of the normal state whereas positive IOD represents conditions nearly opposite to the normal. Therefore, major focus of attention has been to understand pIOD. This article concerns mostly with pIOD events and for simplicity, is referred to as IOD hereafter.

An IOD event can be detected using Dipole Mode Index (DMI) which is defined as the difference in SST anomalies between western and eastern equatorial Indian Ocean (figure 4). Averages of anomalies are calculated for a box in

the western Indian Ocean bounded by  $50^{\circ}\text{E}$ – $70^{\circ}\text{E}$  and  $10^{\circ}\text{S}$ – $10^{\circ}\text{N}$  and in the east by  $10^{\circ}\text{S}$ –Equator and  $90^{\circ}\text{E}$ – $110^{\circ}\text{E}$ . In general, the DMI is expected to be higher than one standard deviation and should remain so for 3 to 4 months, in an IOD year. The west minus east anomalies are positive during a pIOD year and vice versa. During the 1870–1999 period, 27 pIOD events occurred and recent IOD events are 1961, 1963, 1967, 1972, 1982, 1994, and 1997 (Yamagata *et al* 2002; Vinayachandran *et al* 2007). During 2003, a pIOD event was initiated but terminated midway (Rao and Yamagata 2004). Most recently, an IOD event occurred during 2006 (Vinayachandran *et al* 2007). Twenty nIOD events have also occurred during the 1870–1999 period (Meyers *et al* 2007).

Evolution of the IOD (figure 5) is strongly locked to the seasonal cycle due to the thermodynamic air-sea feedback between an atmospheric anticyclone located to the east of Sumatra (Annamalai

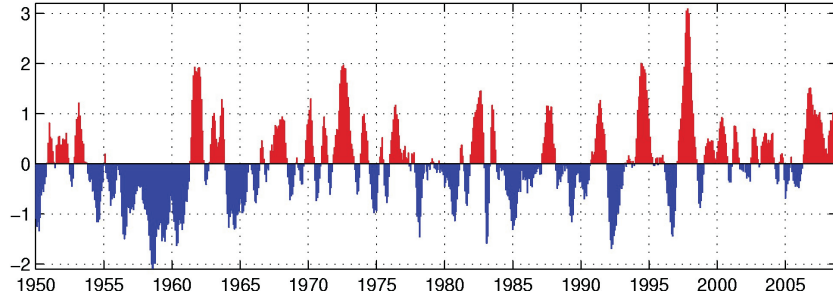


**Figure 4.** The dipole mode index (DMI) defined (Saji *et al* 1999) as the difference in SST anomalies between western ( $50^{\circ}\text{E}$ – $70^{\circ}\text{E}$ ) and eastern ( $90^{\circ}\text{E}$ – $110^{\circ}\text{E}$ ) Indian Ocean. The DMI is normalized by its standard deviation and smoothed by a 5-month running mean before plotting.

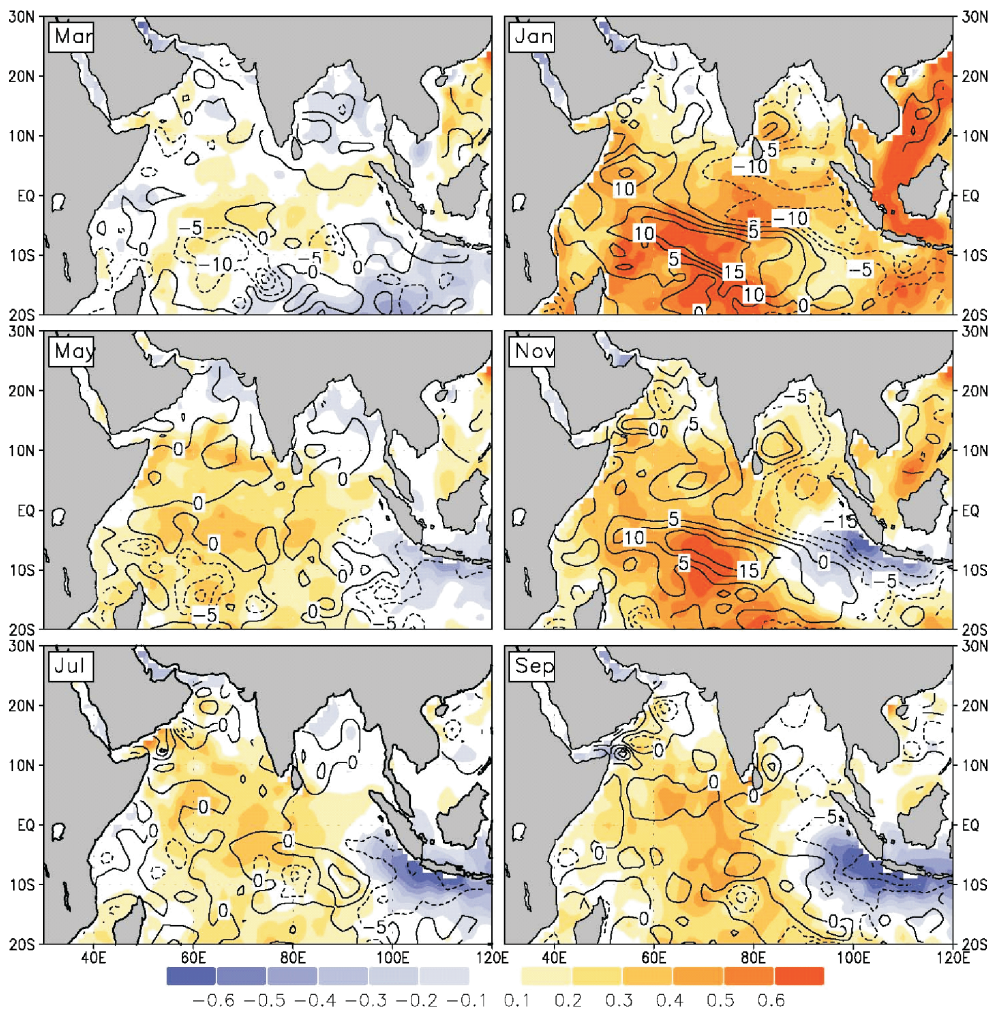


**Figure 5.** Monthly mean composite anomaly patterns of SST and depth of  $20^{\circ}\text{C}$  for the pIOD years. Alternate months starting from March in the pIOD year are plotted. The top right panel corresponds to January of the year following pIOD.

*et al* 2003) and the ocean underneath being dependent on the seasonal cycle of winds (Li *et al* 2003). Typically, an event begins to appear during late spring/early summer, matures during September–November and most of the anomalies disappear by January of the following year. Easterly equatorial wind anomalies and warm SST anomalies

in the central part of the Indian Ocean begin to appear during spring (figure 6). SST anomalies associated with the IOD peak during September–November. For certain events, however, there is a clear indication that the atmospheric component appears much earlier in spring in the form of easterly wind anomalies and southeasterlies

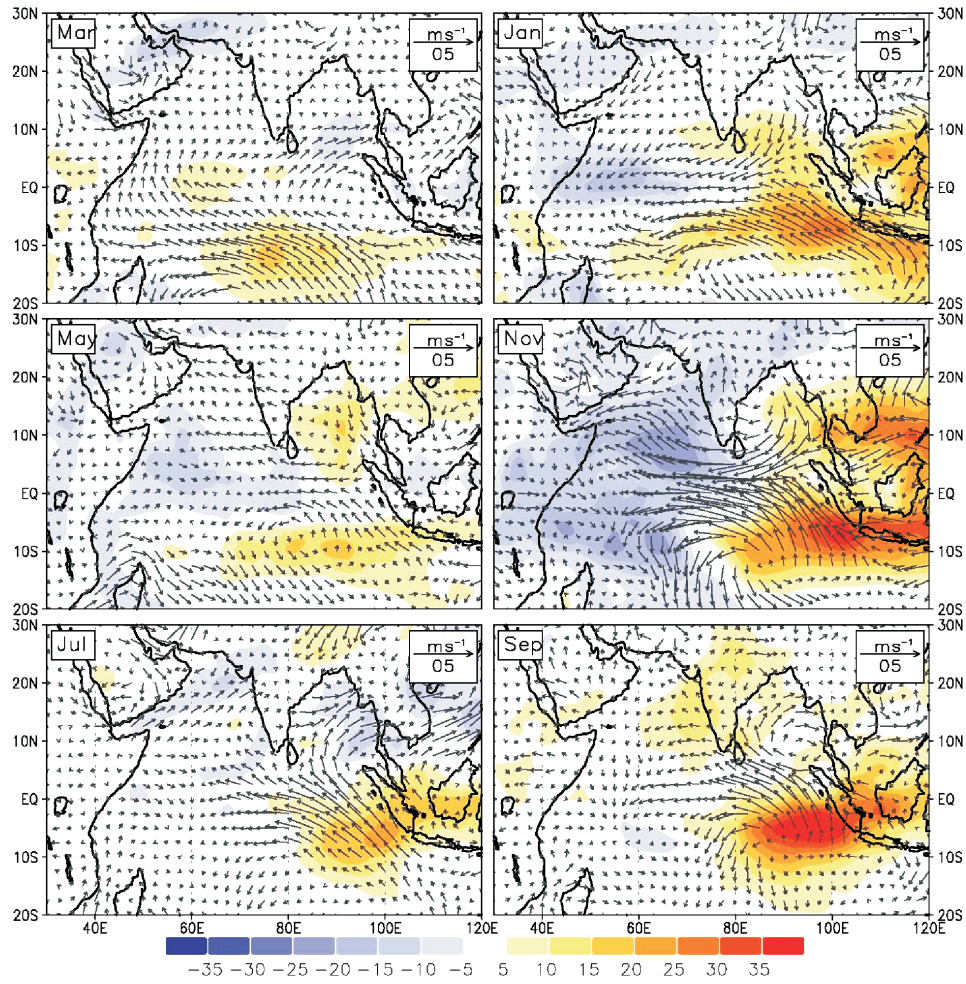


**Figure 6.** Monthly mean composite anomaly patterns of OLR ( $\text{Wm}^{-2}$ , shaded) and surface wind ( $\text{ms}^{-1}$ , vectors) for the pIOD years. Alternate months starting from March in the pIOD year are plotted. The top right panel corresponds to January of the following year of pIOD.

off Sumatra (Vinayachandran *et al* 1999, 2007). Even though the general features of every event are similar, there are differences in the location and timing of the peak anomalies. For example, the peak SST anomalies during the 1994 event occurred about two months earlier compared to the 1997 event. The eastern pole is located more or less in the same region for every event because coastal upwelling is an important cooling mechanism. In the west, however, regions covered by positive anomalies vary considerably between events. During the 2006 event, for example, positive SSTA were located to the west of the commonly considered IOD box bounded by  $50^{\circ}\text{E}$ – $70^{\circ}\text{E}$ ;  $10^{\circ}\text{S}$ – $10^{\circ}\text{N}$  (Vinayachandran *et al* 2007).

Copious upwelling takes place along the eastern coast of the EIO during an IOD which leads to enhanced biological productivity and affects the bio-geochemistry of the region. The satellite data coverage of chlorophyll concentration is restricted to the events of 1997–98 and 2006

(Wiggert *et al* 2009; Iskandar *et al* 2009). During the strong IOD event of 1997–98, the eastern equatorial Indian ocean, which is not usually very productive, experienced phytoplankton blooms (Murtugudde and Busalachhi 1999). This event was also associated with an increase in chlorophyll *a* concentration in the southeastern Bay of Bengal, and a decrease in the southwestern part of the bay (Vinayachandran and Mathew 2003). In the Arabian Sea, influence of IOD led to a decrease in chlorophyll *a* concentration, primary productivity and sea to air  $\text{CO}_2$  flux (Sarma 2006). Chlorophyll concentration in the western Indian Ocean and along the coast of India shows a decrease during the IOD years of 1997 and 2006 (Wiggert *et al* 2006). Enhanced biological productivity off the coast of Indonesia during 1997 led to the death of coral reef in a large area due to the asphyxia caused by the oxidation of organic matter in the water column (Abram *et al* 2003).

Coral records have provided evidences for the presence of IOD in the present as well as in the past because upwelling and cooling taking place in the eastern ocean during IOD events leave their signatures in the marine environment, which are preserved in coral records. Anomalies of Sr/Ca indicate temperature anomalies in the ocean whereas  $\delta\text{O}^{18}$  indicates influence of both temperature and salinity. Such records from Mentawai Islands off Indonesia showed that several IODs occurred in the past, including an event in 1877 which was stronger than that during 1997 (Abram *et al* 2003). On the western side, coral density bands of Malindi Marine Park, Kenya also present evidences of the IOD (Kayanne *et al* 2006). Here, anomalies of  $\delta\text{O}^{18}$  were correlated with the increase in rainfall during IOD events. The Sr/Ca ratio and  $\delta\text{O}^{18}$  (after removing temperature signals) from coral records carry distinct signals of temperature and salinity anomalies respectively, and therefore, can be used for reconstructing past records of IOD (Abram *et al* 2008). Such records show that the IOD during middle holocene were characterized by longer duration of surface cooling caused by enhanced cross equatorial winds.

### 3. Processes

Evolution of SST anomalies involves coupled ocean-atmosphere processes (Vinayachandran *et al* 1999; Murtugudde and Busalacchi 1999; Vinayachandran *et al* 2002). Oceanic processes that are responsible for cooling SST anomalies are: (1) shoaling of thermocline and (2) variations in mixed layer depth. The first process depends chiefly on subsurface ocean dynamics (i.e., coastal and open ocean upwelling), while the second one helps in re-distributing the heat energy in the top few meters of the ocean. Similarly, atmospheric processes that are involved in evolution of SST are (1) atmosphere-ocean heat fluxes and (2) large-scale atmospheric circulations. In order to understand the role of oceans and atmosphere in evolution of SST anomalies during IOD events, we describe oceanic and atmospheric processes separately in this section, focussing on their major contributions to SST anomalies.

#### 3.1 Oceanic processes

Ocean general circulation models (OGCM) have provided useful insights into processes that lead to the development of SSTA during IOD events (Murtugudde *et al* 2000; Vinayachandran 2002). Forced by winds and surface fluxes, they have been able to simulate the evolution of IOD extremely

well (Vinayachandran *et al* 2007). Such models have illustrated that upwelling, forced either by winds or through the propagation of baroclinic waves, is an important process responsible for SST cooling in the east. The semiannual zonal winds over the central equatorial Indian Ocean drive eastward equatorial jets. Anomalies in zonal winds weaken or even reverse the Wyrtki jet, which causes a decrease in eastward transport resulting in a shallow thermocline in the east (Hastenrath *et al* 1993; Vinayachandran *et al* 1999). Along-shore component of winds effectively upwells cooler water to the mixed layer when the thermocline is shallow. Air-sea fluxes also play a significant role in the SST cooling, particularly during initial stages of IOD development (Vinayachandran *et al* 2007). The western warming is mostly controlled by air-sea fluxes and advection by ocean currents. Anomalous downwelling Rossby waves deepen the thermocline which prevents cooling of the SST by entrainment (Murtugudde *et al* 2000). The role of waves is elaborated further below.

#### 3.2 Role of baroclinic waves

The semiannual zonal winds over the central equatorial Indian Ocean excite Kelvin waves which remotely affect sea level variations and thermal structure along the eastern equatorial Indian Ocean (Clarke and Liu 1993; Yamagata *et al* 1996; Meyers 1996). Easterly wind anomalies along the equator drive an anomalous upwelling Kelvin wave which radiates into the eastern Indian Ocean. After reaching the eastern basin they reflect into coastally trapped Kelvin and Rossby waves. This upwelling Kelvin wave lifts up the thermocline in the eastern equatorial Indian Ocean thereby triggering upwelling in the southeastern tropical Indian Ocean (SETIO) (Vinayachandran *et al* 1999; Murtugudde *et al* 2000; Vinayachandran *et al* 2002; Rao *et al* 2002). Local alongshore winds, which are southeasterly during development and peak phase of the Indian Ocean Dipole, also drive the coastal upwelling in the SETIO (Vinayachandran *et al* 1999; Murtugudde *et al* 2000). Due to the strong easterly anomalies along equator and southeasterly winds along Sumatra/Java coasts, strong anomalous anticyclonic wind stress curl forms in the southern tropical Indian Ocean (Xie *et al* 2002). This anomalous wind stress curl forces downwelling Rossby waves in the southern tropical Indian Ocean during developing phase of the IOD (Rao and Behera 2005). Similarly, downwelling Rossby waves are formed in the northern tropical Indian Ocean. In normal years open-ocean upwelling also occurs in the southwestern tropical Indian Ocean forced by negative wind stress curl (Masumoto and Meyers 1998; Xie

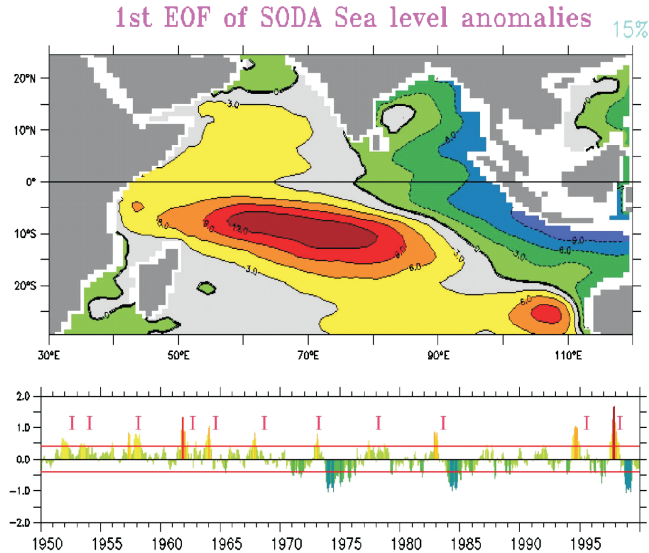


**Figure 7.** First EOF mode of sea level anomalies from SODA (upper panel). Positive Indian Ocean Dipole events are marked as I in the corresponding time series (lower panel).

*et al* 2002). Downwelling Rossby waves radiated from the southeastern Indian Ocean propagate into this upwelling region, deepen the thermocline and warm the SST in the western tropical Indian Ocean (Murtugudde *et al* 2000; Vinayachandran *et al* 2002). These features are brought out clearly in a simple empirical orthogonal function (EOF) analysis of sea level anomalies obtained from SODA (Carton *et al* 2000). The first EOF mode of sea level anomalies clearly shows the structure of Kelvin and Rossby waves in the tropical Indian Ocean. During IOD years, the anomalous upwelling Kelvin waves propagate eastward, reflect and then propagate as coastal trapped Kelvin waves along Sumatra/Java and the Bay of Bengal (figure 7). This results in low sea level anomalies in the eastern equatorial Indian Ocean and the Bay of Bengal. The anomalous downwelling Rossby waves forced by anticyclonic wind stress curl during IOD events are seen as high sea level anomalies with northwest-southeast slope (Rao and Behera 2005).

### 3.3 Role of salinity

Interannual sea surface salinity variations in the Indian Ocean are caused both by freshwater forcing and ocean dynamics (Murtugudde and Busalacchi 1998; Perigaud *et al* 2003; Yu and McCreary 2003; Vinayachandran and Nanjundiah 2009). Interestingly, a coupled model simulation shows that significant interannual salinity variations in the Indian Ocean occur only during IOD years (Vinayachandran and Nanjundiah 2009). Scanty observations of salinity in the tropical Indian Ocean prevent the identification of the

role of salinity on IOD. However, using OGCMs, a few researchers have examined the role of salinity on SST during IOD event. The barrier layer that is present (absent) during normal years in the eastern (western) equatorial Indian Ocean, erodes (forms) during positive dipole years as a response to decreased (enhanced) precipitation (Murtugudde *et al* 2000). This feeds back to the SST in the form of enhanced cooling (warming) due to strong vertical mixing (shallow mixed layer) in the eastern (western) Indian Ocean. Masson *et al* (2004) examined the role of salinity on equatorial currents. The anomalous easterlies over the equator drive south equatorial current at surface and an equatorial under current at subsurface. The south equatorial current transports the normal fresh pool westward, increases stratification and creates a barrier layer in the western equatorial Indian Ocean. As a result of this shallow stratification, wind mixing is restricted and amplitude of the momentum increases in the surface layer, resulting in strengthening of south equatorial current and continuation of equatorial under current (Masson *et al* 2004). These results suggest that there is a positive feedback between salinity and SST in the tropical Indian Ocean during a positive IOD event.

### 3.4 Atmospheric processes

Compared to the southeastern coasts of tropical Pacific and tropical Atlantic Oceans characterized by cold SST tongue and low stratus clouds, the SETIO (off Sumatra) is a region of warm pool (Vinayachandran and Shetye 1991) with deep convection (Li *et al* 2003; Gadgil *et al* 2004). Over a warm ocean such as the tropical Indian Ocean, a modest SST anomaly may induce deep convection *in situ*, so that SST-cloud relation is in phase (Li *et al* 2003). Since, a major part of the tropical Indian Ocean is covered by a warm pool (SST greater than 28°C) (Vinayachandran and Shetye 1991), the SST-cloud relation is in phase. On the other hand, in tropical Pacific, significant phase differences are observed; maximum SST anomalies are observed in the eastern tropical Pacific during a warm ENSO, but maximum anomaly in convection associated with ENSO appears in the central Pacific. In-phase SST-cloud relation in tropical Indian Ocean leads to negative feedback between the atmosphere and ocean. As cloud amounts increase in the tropical Indian Ocean, in response to the increase in SST, the net downward shortwave radiation decreases and cools the SST (Li *et al* 2003). Another thermodynamic air-sea feedback in the SETIO is the Bjerknes feedback mechanism. For example, a drop in SST in the SETIO implies a corresponding drop in cloud amount *in situ*. A decrease in atmospheric

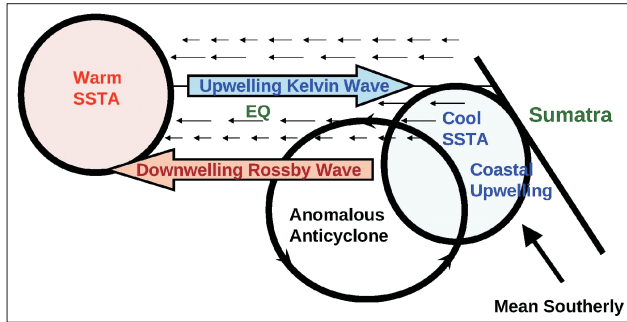


**Figure 8.** Schematic of coupled positive feedback in the southeastern equatorial Indian Ocean. Modified after Li *et al* (2003).

convection leads to development of descending Rossby waves to the west (Gill 1980), resulting in an anomalous anticyclonic circulation to the west of decreased convection center. Since, winds along SETIO are southeasterly during the development phase of IOD, the anticyclonic circulation enhances wind speeds in the SETIO. The enhanced winds, in addition to driving coastal upwelling and vertical mixing, induce strong evaporative cooling of the sea surface, leading to more cooling of the SETIO (figure 8). This positive feedback acts only during boreal summer, as mean winds along SETIO reverse in the fall. During strong IOD years (such as 1994 and 1997), seasonal southeasterlies associated with the Asian summer monsoon reinforce coastal upwelling associated with the IOD near Sumatra in boreal summer and fall, assisting in initiation and strengthening of these events (Halkides *et al* 2006). On the other hand, boreal fall equatorial westerlies deepen the thermocline in the eastern basin, reducing the cold SSTAs in the eastern equatorial region and near Sumatra and Java. Such a process contributed to the early termination of the 1994 IOD. Seasonal reversal of monsoon winds during boreal winter reduces coastal upwelling along Sumatra and Java, contributing further to IOD termination.

### 3.5 Intraseasonal oscillation

Madden and Julian (1972) first reported variability at time scales of 30–60 day in zonal winds and convection, popularly known as MJO. Anomalous convection first develops in western tropical Indian Ocean, propagates eastward across the Indian Ocean and maritime continent, and then decays east of 180°E. Associated with the propagating anomalous convection, baroclinic circulation anomalies in the wind field are excited; easterlies (westerlies) to the east (west) of the anomalous convection in the lower (upper) troposphere. In the suppressed convection phase of MJO, baroclinic circulation anomalies also occur in the atmosphere with opposite directions. The MJO

activity becomes weak during IOD years in response to the strong subsidence in the SETIO (Rao and Yamagata 2004). During pure IOD events, MJO appears before the termination of IOD and the associated westerlies, anomalous downwelling Kelvin waves and deepens the thermocline in the SETIO, arresting air-sea coupling. Suppressed convection phase of MJO, associated with equatorial easterly wind anomalies, can trigger an IOD event by exciting anomalous upwelling Kelvin waves (Han *et al* 2006; Rao *et al* 2009). Their model simulations suggested that before the onset of the strong 1997 dipole, basin-wide wind-driven oceanic resonance with a period near 90 days, involving the propagation of equatorial Kelvin and first-meridional-mode Rossby waves across the basin, was excited. Associated with the resonance was a deepened thermocline in the eastern basin during August and early September, which reduced the upwelling in the eastern anti-node of the IOD, thereby delaying the reversal of the equatorial zonal SST gradient – an important indicator of a strong IOD – by over a month compared to 1994 IOD event.

## 4. Dependence of IOD on El Niño

### 4.1 Observations

The mean thermocline in the Indian Ocean is deep, compared to the Pacific. Therefore, initiation of a coupled phenomenon that involves shallowing of the thermocline (so that the subsurface ocean can interact with the SST through wind mixing) is considered to be an uphill task. This conviction led to the tenet that the Indian Ocean is passive and merely responds to the atmosphere (Kiladis and Diaz 1989; Venzke *et al* 2000; Alexander *et al* 2002), and interannual variability of the Indian Ocean SST are forced mainly by ENSO, through an atmospheric bridge (Klein 1999; Alexander *et al* 2002). The bridge is through Walker circulation which, climatologically, has ascending motion over the western Pacific and maritime continent, and descending motion over eastern Pacific. This normal Walker cell reverses during ENSO, with strong descending motion over western Pacific and equatorial Indian Ocean. About 4 months after large-scale SST anomalies are observed in the equatorial Pacific, the whole of the Indian Ocean is covered with SST anomalies of the same sign. The warming (cooling) of the Indian Ocean during warm (cool) phase of ENSO is usually basin-wide and mainly due to surface heat fluxes (Klein *et al* 1999; Venzke *et al* 2000). The 4 month delay for the Indian Ocean to warm in response to ENSO is due to the thermal inertia of the ocean surface layer. The Indian Ocean

warming associated with ENSO, however, is not basin-wide at all stages of ENSO. In the early stages of development of an ENSO, there are cold SSTA in the eastern equatorial Indian Ocean but they disappear as El Niño matures (Rasmusson and Carpenter 1982; Huang and Kinter 2002; Hendon 2003; Krishnamurthy and Kirtman 2003).

Simultaneous correlations between SSTA in the eastern Indian Ocean and ENSO indices tend to suggest that IOD events are forced by ENSO (Allan *et al* 2001; Baquero-Bernal *et al* 2002; Xie *et al* 2002; Hastenrath 2002; Krishnamurthy and Kirtman 2003; Annamalai *et al* 2003). The strong IOD event of the recent times that occurred during 1997 coincided with a very strong ENSO. However, IODs have occurred together with ENSO as well as independently, and SSTA caused by ENSO lack the dipole pattern as during the IOD events. Moreover, anomalies associated with IOD are phase-locked to the seasonal cycle, they appear during boreal summer and fall, whereas, basin-wide anomalies associated with ENSO appear mostly during winter and spring (Tozuka *et al* 2008). EOF of SST anomalies shows a basin-wide pattern as the first mode due to the effects of ENSO. The second mode, on the other hand, shows remarkable sea-saw between the eastern and western Indian Ocean which is due to the IOD and this mode is independent of ENSO (Yamagata *et al* 2004). About 50 percent of the IOD events have occurred together with ENSO and the rest independently (Saji and Yamagata 2003; Meyers *et al* 2007). Clearly, the ocean-atmosphere coupling intrinsic to the Indian Ocean can lead to the development of an IOD event (Saji *et al* 1999; Yamagata *et al* 2003, 2004; Behera *et al* 2006; Chang *et al* 2006; Schott *et al* 2009).

#### 4.2 Coupled models

Coupled ocean-atmosphere general circulation models have been successful in reproducing the IOD events, as illustrated first by Iizuka *et al* (2000) and characteristics of IODs simulated by coupled models are comparable to that seen in observations (Iizuka *et al* 2000; Baquero-Bernal *et al* 2002; Lau and Nath 2004; Cai *et al* 2005; Behera *et al* 2006; Song *et al* 2007). The major issue that has been addressed using such models is to test whether IOD is generated by processes intrinsic to the Indian Ocean or by external forcing from the Pacific.

In a coupled simulation for 50 years (Iizuka *et al* 2000), the model generated 8 IODs compared to 20 IOD events in a 100 year simulation using CCSM 2 (Vinayachandran and Nanjundiah 2009). Iizuka *et al* (2000) found poor correlation between DMI and SSTA in the NINO3 region and concluded that the IOD in this model is

independent of ENSO. Bequero-Bernal *et al* (2002) carried out two simulations using a coupled model, first with effects of El Niño included and then excluded. They concluded that dipole like variability in the model is forced primarily by ENSO but they also found that the model additionally generates a dipole structure forced by atmospheric fluxes, independent of ENSO. The SINTEX model simulation had 20 IODs in its 80 year model integration (Gualdi *et al* 2003). The peak model SSTA associated with the IOD occurred about 3 months before the SSTA peak in the NINO3 region suggesting that IOD evolution in the model is generally independent of ENSO. However, the model results suggested that sea level pressure anomalies associated with ENSO might produce atmospheric conditions that are favourable for the generation of IOD. In the GFDL coupled model simulations (Lau and Nath 2004), IOD pattern was caused primarily by ENSO; changes in surface wind field over the Indian Ocean associated with ENSO modify both air-sea fluxes and oceanic process leading to dipole SST pattern. The model also produced strong IOD events in the absence of ENSO and these were caused by an annular mode associated with sea level pressure anomalies south of Australia. Using the SINTEX model, Fischer *et al* (2005) carried out a coupled model experiment in which the effect of ENSO was suppressed by constraining wind stress over tropical Pacific. The IOD in this simulation was identical to the run that included ENSO. Modifying the SST field to suppress ENSO (Behera *et al* 2006) in the same model yielded a similar result. The IOD events in the GFDL CM2.1 coupled model are preceded by anomalous conditions in the west Pacific warm pool, marked by an eastward shift in convection, westerly winds and SST (Song *et al* 2007) suggesting that variations in Indo-Pacific warm pool are crucial for generating IOD conditions. From process experiments, they concluded that IOD forms as a result of processes intrinsic to the Indian Ocean. They also noted that IODs can also be caused by ENSO even though the number of cases of the latter is relatively smaller. The CSIRO Mark 3 coupled model produced 74 ENSO and 34 IOD events out of 240 years of model simulation (Cai *et al* 2005). Among these, there were only occasional coincidence of IOD and ENSO, whereas 23 IOD events occurred one year after ENSO. Unrealistic interactions between the Indian and Pacific Oceans lead to development of such IOD events (Cai *et al* 2005) suggesting that mechanism that leads to the formation of IOD like events in coupled models needs further investigation.

In summary, both observations and models agree that it is not necessary to have forcing by ENSO in order to generate an IOD. That

is, the Indian Ocean can support its own air-sea interaction process. A crucial role in the evolution of the IOD is played by the interaction of the thermocline with the SST. The slope of the thermocline in coupled models show considerable variation between models (Saji *et al* 2006) and the frequency of occurrence of IOD in these models is crucially dependent on the shape of the thermocline. In ocean-atmosphere coupled models, dynamical coupling takes place through wind stress and thermodynamic coupling through SST and air-sea heat flux. Thus generation of ENSO in a coupled model can be suppressed by not allowing the atmosphere to interact with the model SST. This is typically achieved by replacing model SST with climatology (Elliot *et al* 2001; Bequero-Bernal *et al* 2002; Behera *et al* 2005). The dynamical coupling through wind stress is present in such experiments, which can produce a Bjerknes type of feed back in the presence of a shallow thermocline. Consequently, oceanic variability associated with ENSO is not well suppressed and influences oceanic regions in the SETIO (Fischer *et al* 2005). A second method also has been used (Fischer *et al* 2005), in which, the dynamical coupling is suppressed by prescribing climatological wind stress in the tropical Pacific. This constraint removes the atmospheric signals associated with ENSO and reduces the oceanic signals dramatically (Fischer *et al* 2005). Considering that oceanic processes associated with the IOD can evolve even in the absence of Indonesian through flow (ITF) (Vinayachandran *et al* 2007), the latter method could be considered as the preferred mode of suppressing ENSO in coupled models.

## 5. Triggering

Evolution of the 1997–98 event together with an El Nino prompted the hypothesis that ENSO can induce contrasting wind anomalies in the equatorial Indian Ocean which can mature into an IOD (Ueda and Matsumoto 2001). This mechanism, however, is not capable of explaining all IODs, particularly those formed during non-ENSO years. Signatures of IOD events begin to appear in spring (March–April) and therefore, several studies have explored a mechanism that could induce easterly wind anomalies along the equator and southeasterlies off Sumatra. Spring rainfall in the eastern equatorial Indian Ocean (EEIO) is simultaneously correlated with the west-central Pacific SSTA and unrelated to local SSTA (Annamalai *et al* 2003). Based on this, Annamalai *et al* (2003) have proposed that initiation of the IOD takes place in boreal spring which is the time window through which external forcing from the Pacific

can influence the Indian Ocean. In this mechanism, warm SSTA in west-central Pacific modifies the Walker circulation and leads to subsidence over the EEIO and the IOD grows by the Bjerknes feedback. However, their experiments with an AGCM showed rather weak response of the EEIO rainfall to west-central Pacific SSTA and no attempt was made to demonstrate that SST and thermocline depth anomalies evolve into conditions favourable for the IOD. According to Kajikawa *et al* (2001), intensification of the Hadley cell over the western Pacific can enhance the southeasterly in the EEIO, SST cooling and suppression of convection, triggering an IOD. The intensification takes place during summer and can be either due to ENSO or monsoon. However, wind anomalies associated with the IODs appear during spring (Vinayachandran *et al* 1999, 2007) which the above mechanism fails to explain.

Fischer *et al* (2005) examined triggering mechanisms of IOD in the presence as well as absence of El Nino using a coupled model. In the presence of ENSO, as the convection shifts eastward in the Pacific during the development of ENSO, easterly wind anomalies occur in the eastern Indian Ocean and the thermocline becomes shallow. This is followed by development of upwelling favorable winds and reduced precipitation, triggering the growth of an IOD. In the absence of ENSO, the trigger originates from an anomaly in Hadley circulation during April–May featuring southerly cross equatorial winds and reduced rainfall in the SETIO, completely independent of atmospheric and oceanic processes in the Pacific. Interestingly, these are preceded by anomalies of SSTA in March–April suggesting that the trigger originates in the ocean.

In quite a deviation from all other theories, Francis *et al* (2007) proposed that cyclones over the Bay of Bengal during spring season can trigger IOD events. Initiation of suppressed convection in the SETIO is caused by meridional pressure gradients created by severe cyclones over the bay. The development of this anomalous convection into IOD is effected by the fact that suppression of convection in the east is associated with enhancement of convection in the west (Gadgil *et al* 2003, 2004), the former leading to southeasterlies off Sumatra and easterlies over EIO.

IOD events are preceded by a downwelling Rossby wave that originates from the eastern boundary (Vinayachandran *et al* 2002). These waves precondition the western equatorial Indian ocean by deepening the thermocline. Such wave propagations during 1993 and 1996 provided a favourable background for the evolution of the IOD events during 1994 and 1997, respectively. Rossby waves can also excite a Kelvin wave which

preconditions the thermocline in the eastern Indian Ocean as in the case of 2003 and 2006 (Rao *et al* 2009). Intensification of the northward portion of the ITCZ in March or a suppressed convection phase of an MJO can also restrict convection, triggering an IOD (Rao *et al* 2009).

A key parameter involved in the coupled ocean atmosphere interaction culminating in the IOD is depth of the thermocline (Li *et al* 2003). A shallow thermocline in the east is a necessary condition for upwelling to work efficiently to cool the SST (Vinayachandran *et al* 1999, 2002, 2007; Murtugudde *et al* 2000). Therefore, preconditioning of thermocline provides a favourable background, and, probably, a necessary condition for the formation of IOD (Annamalai *et al* 2005). The pre-conditioning of the Indian Ocean can be caused by Pacific decadal variability, which can influence the Indian Ocean either through atmosphere or through the ITF (Annamalai and Murtugudde 2004). The former is effected through zonal wind anomalies along the equator and an anticyclone to the east of Sumatra, and the latter by the influence of ITF on the thermocline (Annamalai *et al* 2005). Consequently, IOD events are stronger in decades during which Pacific decadal variability favors a shallow thermocline in the SETIO such as the 1960s and 1990s.

Being a coupled ocean-atmospheric process, triggering of an IOD can originate either in the ocean or in atmosphere. All the studies mentioned above, except Rao *et al* (2009), point to a trigger from the atmosphere, either by a modification of the Walker circulation or of the Hadley cell. This is consistent with evolution of IOD events in the last decade; observations suggest that first signs of the IOD appear as anomalous easterlies along the equator and anomalous southeasterlies off Sumatra (e.g. the 2006 IOD event (Vinayachandran *et al* 2007)). Shallowness of the thermocline is crucial for further development of the IOD as it is a crucial parameter for the Bjerknes feedback. There is a near-perfect sea-saw relationship in convection between the eastern and western boxes of IOD; whenever convection is enhanced in the eastern side, it is suppressed in the west and vice versa (Gadgil *et al* 2003, 2004). Thus, once the thermocline is preconditioned, enhancement of convection either in the west or in the east can trigger a positive feedback.

## 6. Influence of the Indian Ocean dipole in regional climate system

### 6.1 IOD and east African rainfall

The variability of east African rainfall has profound impact on the livelihood of millions of people in

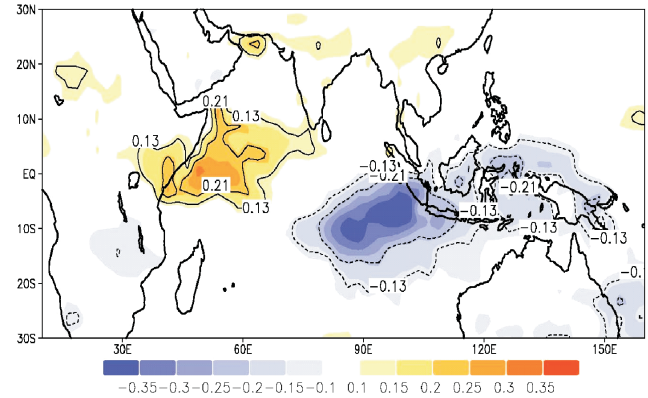


**Figure 9.** Correlation between DMI and precipitation over the Asian monsoon region. DMI is computed using HadISST available at (<http://badc.nerc.ac.uk>) and precipitation used is CPC merged analysis of precipitation (CMAP) available at <http://iridl.ldeo.columbia.edu>.

the developing countries in this region, who mainly depend on the rain-fed agriculture and regional fisheries. Relationship between the SST in the tropical Indian Ocean and the climate in the surrounding regions has been explored by several studies even prior to the discovery of the IOD (Saha 1970; Reverdin *et al* 1986; Nicholls 1995; Nicholson and Kim 1997; Goddard and Graham 1999). Many of these studies focused on the anomalous convection and rainfall in the east African countries in 1961/62 and attributed it to the anomalously warm western equatorial Indian Ocean. In general, the influence of Indian Ocean SST tends to dominate in the rainfall variability of Africa in the warm phase of ENSO and the Atlantic Ocean controls the rainfall of Africa in the cold phase (Nicholson and Kim 1997). Experiments with atmospheric general circulation models to quantify the relative influence of the Indian and Pacific Oceans suggest that even though the Pacific SST anomalies influence the rainfall activity in the African region, atmospheric response to the Indian Ocean variability is essential for the simulation of correct rainfall response over central, southern and eastern Africa, particularly the simulation of observed central-eastern/southern African dipole pattern in rainfall (Goddard and Graham 1999). Interestingly, there are some studies, which suggest that the teleconnection between the east African rainfall and ENSO is a manifestation of a link between ENSO and the IOD (Black *et al* 2003).

After discovery of the IOD (Saji *et al* 1999; Webster *et al* 1999), several studies have investigated the role of IOD on regulating regional climate. There is a tendency for increased rainfall in the tropical eastern Africa and drought in Indonesia in IOD years (Saji *et al* 1999). The correlation between the DMI and precipitation over the Asian monsoon regime confirms this (figure 9).

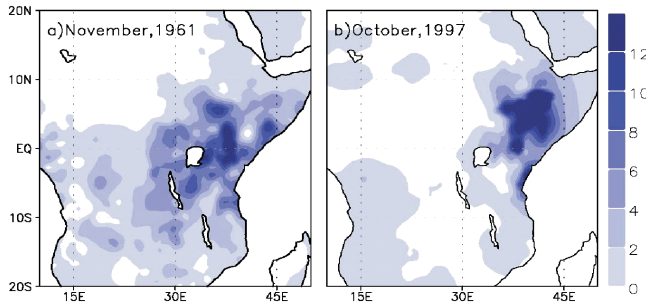


**Figure 10.** Rainfall maps for Africa in a) November 1961 and b) October 1997. Rainfall data used is global gridded station rainfall data (Chen *et al* 2002), available at <ftp://ftp.cpc.ncep.noaa.gov/precip/50yr/gauge/0.5deg>.

The extreme floods in East African countries in 1961–62 and 1997–98 (figure 10) were associated with anomalous conditions in the Indian Ocean (Saji *et al* 1999; Webster *et al* 1999; Birkett *et al* 1999; Saji and Yamagata 2003). Extreme flood conditions in the east-African region in 1997–98 cannot be attributed to an *exaggerated response* to the El Nino as the correlation between the east African rainfall and the central Pacific SST is only 0.24 (Webster *et al* 1999; Latif *et al* 1999). Further, a similar flood in 1961–62 did not co-occur with an El Nino. Enhanced rain in the east African region is associated with increased moisture convergence due to strong westerlies over the central Africa and easterlies from the equatorial Indian Ocean as a response of warm western pole of the IOD (Ummenhofer *et al* 2009). SST anomaly in western pole of the IOD has more impact on the east African short rains compared to that of the east pole (Ummenhofer *et al* 2009), these SST anomalies result from the strong sub-surface influence due to propagating Rossby waves related to the IOD events (Rao and Behera 2005). This slowly propagating air-sea coupled mode could be an indicator for the prediction of the IOD induced short rain events well in advance. Atmospheric and coupled ocean-atmosphere general circulation models have been able to simulate the observed association between the DMI and east African rainfall reasonably well (Behera *et al* 2003; Conway *et al* 2006). Hence coupled models also may be used to predict east African short rains.

### 6.2 IOD and Indian summer monsoon rainfall

A major advance in our understanding of the interannual variation of the Indian summer monsoon rainfall (ISMR) occurred during the 1980s, with the discovery of a strong link with El Nino and Southern Oscillation (ENSO), the dominant signal of interannual variation of the coupled ocean-atmosphere system over the Pacific (Sikka 1980; Pant and Parthasarathy 1981; Rasmusson and

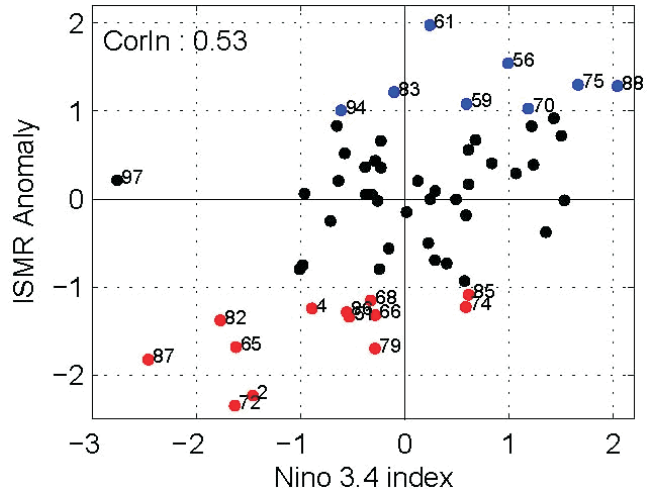


**Figure 11.** Scatter diagram of normalized ISMR anomaly versus Nino 3.4 SST anomaly. Both anomalies are normalized by their respective standard deviations. ISMR data is obtained from <http://tropmet.res.in> and NINO 3.4 index is obtained from <http://www.cpc.noaa.gov/data/indices/sstoi.indices>.

Carpenter 1983). There is a high propensity of deficit monsoon during warm ENSO events, with deficit in 21 out of 25 such events during 1875–1979, which included 9 of 11 seasons with largest anomalies (Rasmusson and Carpenter 1983). It can be seen from figure 11 that this is true in general. However, while majority of the droughts are associated with a positive Nino 3.4 index (El Nino condition), there are droughts of 1974 and 1985 which are associated with negative SST anomaly in the Nino 3.4 region. The NINO 3.4 index is very small in the drought years such as 1966, 1968 and 1979. Again, while in majority of the excess monsoon seasons, SST anomaly in the Nino 3.4 region is negative (La Nina condition), it is positive in 1983 and 1994. Further, in 1997, during the strongest El Nino year in the century, the ISMR was above normal. Consequently, Kumar *et al* (1999) suggested that the relationship between the Indian monsoon and ENSO had weakened in the recent decades.

The correlation between DMI and ISMR is rather weak (figure 9). However, if we consider case by case, out of the 11 intense (anomalies in DMI more than one standard deviation) positive IOD events that occurred during 1958–1997, eight events (1961, 1963, 1967, 1977, 1983, 1994, 1993 and 1997; i.e. 73% of the positive IOD events during this period) are associated with positive anomalies of the concurrent ISMR (Ashok *et al* 2001). Similarly, out of the three negative IOD events during 1958–97, two events (1960 and 1992) correspond to negative anomalies of the ISMR. Interestingly, the sliding correlation between the ISMR and ENSO has an opposite tendency to that between

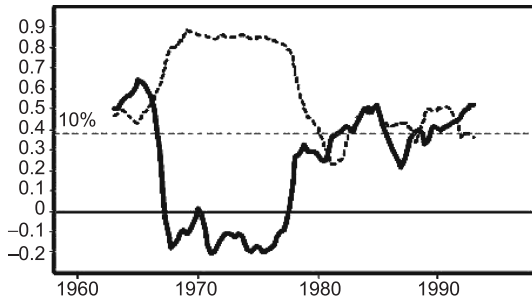


**Figure 12.** 41-month sliding correlations between NINO3 index and ISMR (dashed curve, multiplied by  $-1$ ) and DMI and ISMR (solid curve). Correlation coefficient of 0.38 is significant at 90% (after Ashok *et al* 2001).

ISMР and IOD; i.e., when the ISMR-ENSO (negative) correlation is strong, ISMR-IOD (positive) correlation is weak. Similarly, when the ISMR has a strong positive correlation with IOD, the relation between ENSO and ISMR is weak as seen from figure 12. This strong positive relation between the IOD and ISMR during 1960s and 1990s could be one of the reasons for excess monsoon seasons in 1961, 1994 and near normal monsoon in 1997. However, neither the ENSO nor the IOD can explain all the excess/droughts in the Indian summer monsoon. For example, drought years of 1985 and 1974 are not associated with negative IOD or El Nino. The droughts during 1966, 1968, and 1979 are associated with very small SST anomalies in the central Pacific and no IOD signal in the Indian Ocean. Hence, even though a few modeling studies with AGCMs and coupled OAGCMs also suggest that the positive IOD events can intensify the Indian summer monsoon rainfall (Ashok *et al* 2001, 2004; Guan and Yamagata 2003; Guan *et al* 2003), we still need to understand the role of IOD in the interannual variation of the ISMR.

### 6.3 ISMR and equatorial Indian Ocean oscillation

The extreme drought in 2002 and the very fact that none of the predictions (irrespective of whether it is using complex GCMs or empirical models) could anticipate this drought, triggered debates among researchers around the world on the factors influencing the ISMR variability. This drought was neither associated with a very strong El Nino or a negative IOD event (Gadgil *et al* 2002). Subsequent to this monsoon failure, in 2003, the ISMR was very close to its long term mean. Interestingly, the July mean outgoing longwave radiation (OLR) (which may be used as a proxy for tropical convection) pattern over the Indian region and the equatorial Indian Ocean in 2003 was exactly opposite to that in 2002 (figure 13a & b). In 2002, there was a high OLR anomaly over the western

part of the Indian region and the western equatorial Indian Ocean (WEIO). At the same time OLR anomaly was negative (indicating more convection) over the EEIO. The pattern was just the opposite in 2003. These are not isolated events. In fact, the OLR anomaly patterns in the monsoon months of 1986 and 1994 are quite similar to that in 2002 and 2003, respectively (figure 13c & d). Gadgil *et al* (2004) termed this oscillation in the convection over the WEIO and EEIO as the equatorial Indian Ocean oscillation (EQUINOO). They suggested that the winds along the equatorial Indian Ocean could be considered as a measure of the intensity of the EQUINOO as it responds to the pressure gradient associated with differential heating in the atmosphere due to the difference in convection. EQUINOO index (EQWIN) is defined as the negative of zonal wind anomaly over central equatorial Indian Ocean (averaged over  $60^{\circ}\text{E}$ – $90^{\circ}\text{E}$ ,  $2.5^{\circ}\text{S}$ – $2.5^{\circ}\text{N}$ ). The IOD is a coupled phenomenon and its signatures are seen in convection and surface wind over the equatorial Indian Ocean also (Saji *et al* 1999). Interestingly, there are occasions on which such convection and surface wind anomalies are present without an SST dipole signal (Francis 2006). Hence, even though all the IOD events are associated with EQUINOO, the reverse is not necessarily true.

When the relative influence of EQUINOO and IOD on ISMR is considered, the ISMR is better correlated to the EQUINOO than IOD (Gadgil *et al* 2004). The relation of ISMR with EQWIN and DMI is shown in figure 14a&b. The DMI-ISMR correlation is only 0.05. On the other hand, EQWIN-ISMR correlation is significantly high (0.45). While the ISMR is negatively correlated to the OLR over the WEIO, it is positively correlated to OLR over the EEIO (figure 15). Hence, an excess (drought) monsoon is associated with enhanced (suppressed) convection over the WEIO and suppressed (enhanced) convection over the EEIO. In other words, a positive EQUINOO is favourable for Indian monsoon and a negative EQUINOO highly unfavourable. All the excess/drought monsoon seasons in the period 1958–2003 are associated with the favourable/unfavourable phase of either ENSO or EQUINOO or both (Gadgil *et al* 2004). There is a clear separation between excess and drought seasons when represented in the phase plane of the EQWIN and ENSO indices (which is the negative of normalized SST anomaly in the NINO3.4 region) as shown in figure 16. The linear reconstruction of ISMR on the basis of multiple regression from NINO3 index and the zonal wind over the equatorial Indian Ocean better specifies the ISMR than the regression with only NINO3 index (Ihara 2007). Clearly, monitoring and predicting the EQUINOO and IOD is essential for the

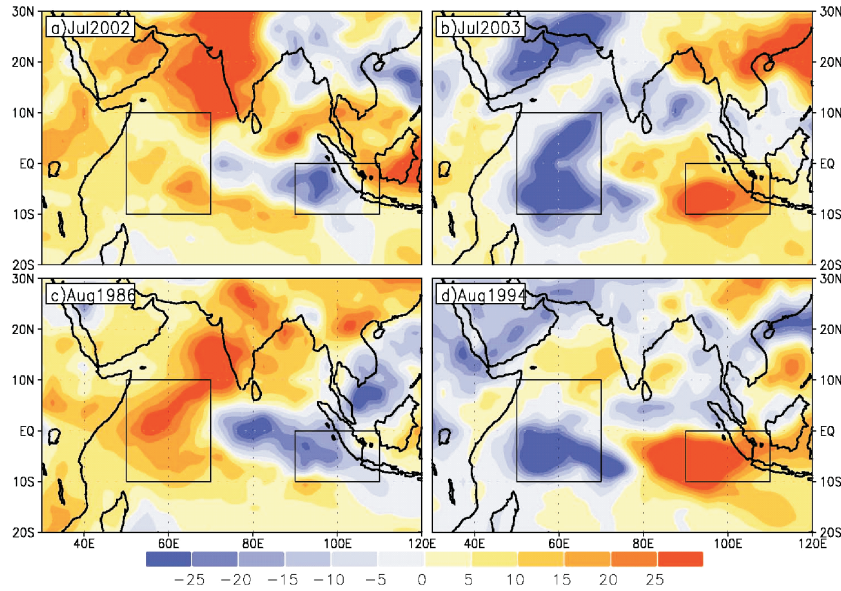


**Figure 13.** NOAA AVHRR OLR ( $\text{Wm}^{-2}$ ) anomaly patterns for a) July 2002, b) July 2003, c) August 1986 and d) August 1994. Data is obtained from <http://www.cdc.noaa.gov>.

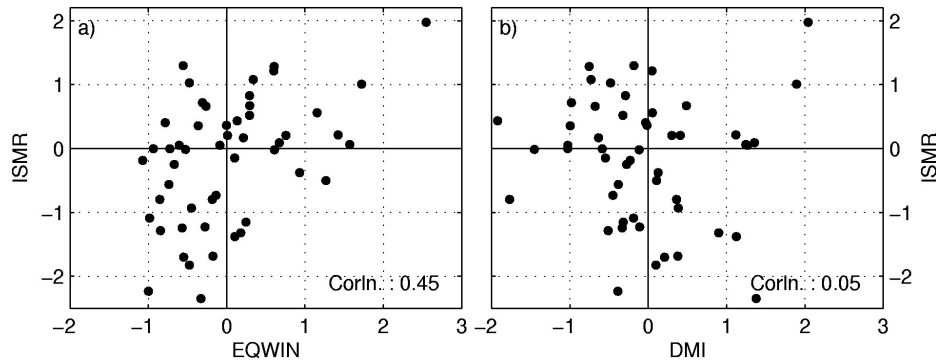


**Figure 14.** Scatter plot of ISMR versus a) EQWIN and b) DMI. EQWIN is computed from the monthly mean surface wind data from NCEP reanalysis, available at <http://www.cdc.noaa.gov>.

prediction of the ISMR. Even though the association between the EQUINO and the extremes of ISMR is now established, the mechanism by which the EQUINO influences the Indian monsoon is yet to be understood. One explanation for the increased rainfall in activity over the Indian region during the positive IOD event is through the enhanced cross-equatorial flow to the Bay of Bengal due to the strong meridional SST gradient across the EEIO (Guan 2003). However, during most of IOD events, the largest precipitation and convection anomalies are observed in the western part of the country (figure 13). More focused research is required to address this problem.

#### 6.4 IOD and Australian rainfall

The years of extensive Australian drought were associated with generally low SST in the low latitudes of eastern Indian Ocean (Streten 1981, 1983). The rainfall over much of Australia tends to be

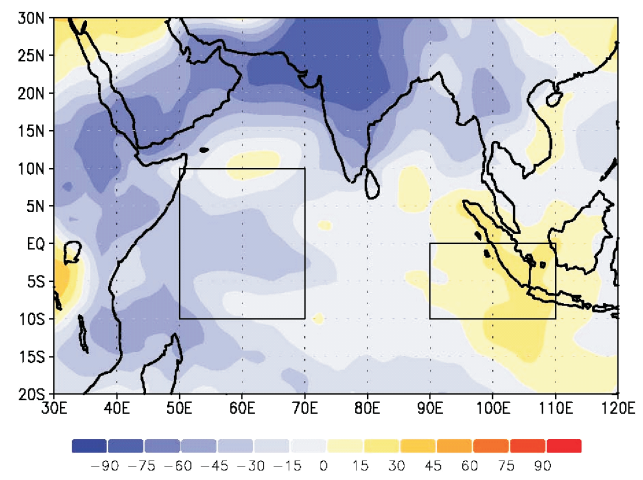


**Figure 15.** Correlation between ISMR and OLR over the Indian monsoon region. Since lower OLR values correspond to deeper convection, negative correlation implies enhanced (suppressed) convection associated with above normal (below normal) ISMR.

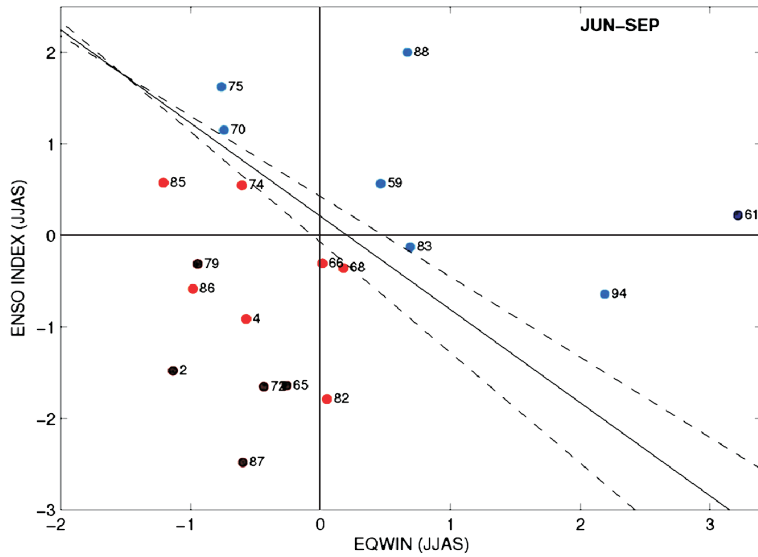


**Figure 16.** Extremes of the ISMR is represented in the phase-plane of EQWIN and ENSO index (both indices are normalized by their respective standard deviations) in the period 1958–2008. Color code: dark red, red, blue and dark blue closed circles represent ISMR anomaly larger than  $-1.5$  standard deviation, between  $-1.5$  and  $-1$  standard deviation, between  $1$  and  $1.5$  standard deviation, and larger than  $1.5$  standard deviation, respectively. Adapted from Gadgil *et al* (2004).

below average during El Niño events (Ropelewski and Halpert 1987). However, in some El Niño events (such as 1986/87), Australian rainfall anomalies are weak or of limited extent while in others (such as 1982/83), the anomalies are major and widespread (Nicholls 1989). The first pattern of the principal component analysis of Australian winter rainfall shows a broad band stretching from the northwest to southeast corners. This is best related to the difference in SST between the Indonesian region and the central Indian Ocean (Nicholls 1989), which is in fact very strong during the IOD years. This suggests that the El Niño events that co-occur with IOD are generally associated with severe droughts in Australia. The negative correlation between the Australian rainfall and Indian Ocean variability has been successfully simulated by AGCMs (Ashok *et al* 2003; Ummenhofer *et al* 2008). Cold SST anomalies prevailing west of the Indonesian archipelago during the IOD events introduce an anomalous anticyclonic circulation at lower levels over Australia, which in turn reduce the rainfall activity over this region (Ashok *et al* 2003).

### 6.5 IOD and intraseasonal oscillations

An active MJO is characterized by slow eastward movement of stronger than average precipitation and westerly winds (Madden and Julian 1972). In summer monsoon months (June–September), rainfall and wind anomalies also propagate northward on intraseasonal time scale over India, southeast and east Asia and the adjacent oceans (Sikka and

Gadgil 1980; Yasunari 1980). Both these propagations are strongly modulated by the IOD (Shinoda and Han 2005; Ajayamohan *et al* 2008, 2009). During the active phase of IOD no significant intraseasonal oscillations occur in Indian Ocean equatorial zonal winds (Rao and Yamagata 2004) and 6–90 day oscillations in winds and OLR tend to weaken (Shinoda and Han 2005). During negative dipole years, submonthly (6–30 day) convection generated in the southeast Indian Ocean is associated with a cyclonic circulation. These submonthly disturbances propagate southwestward, which generate equatorial westerly winds in the eastern and central Indian Ocean and northwesterlies near the coast of Sumatra. During large positive dipole years, submonthly convective activity is largely suppressed in the southeast Indian Ocean and thus no equatorial westerly is generated. The poleward propagation of intraseasonal oscillations during summer monsoon is coherent (incoherent) from  $5^{\circ}\text{S}$  to  $25^{\circ}\text{N}$  during negative (positive) IOD years (figure 17). The mean structure of moisture convergence and meridional specific humidity distribution undergoes radical changes in contrasting IOD years, which in turn influences the meridional propagation of boreal summer intraseasonal oscillations (Ajayamohan and Rao 2008; Ajayamohan *et al* 2009).

### 6.6 IOD and other global teleconnections

The influence of IOD on other global climate systems is far less explored. One major difficulty is that many of the positive IOD events in the recent

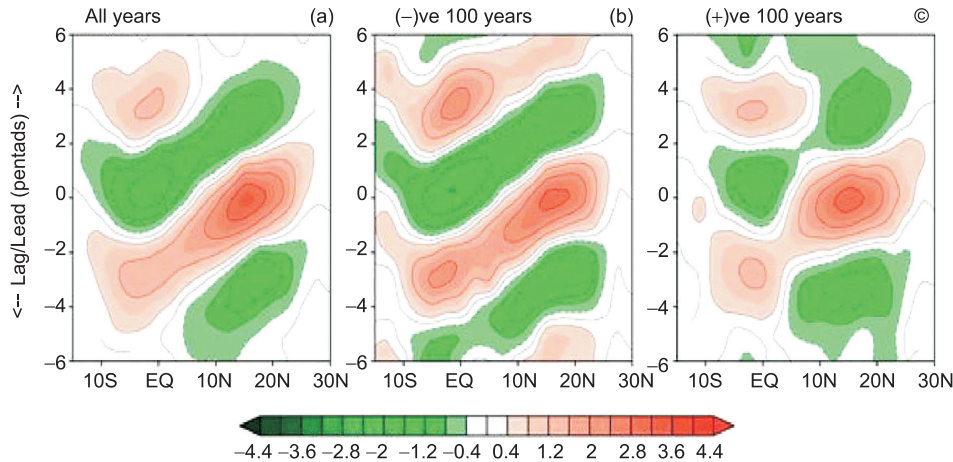


**Figure 17.** (a) Regressed filtered anomalies of CMAP precipitation ( $\text{mm day}^{-1}$ ) averaged over  $70\text{--}95^\circ\text{E}$  as a function of latitude and time lag during the 1980–2004 period. As in (a) but for (b) negative and for (c) positive IOD years. Contour interval is 0.6. Only statistically significant (0.1 significance level using a t test) anomalies are plotted (taken from Ajayamohan *et al* 2008).

years are associated with strong El Nino events and it is difficult to separate the influence of IOD from El Nino. Nevertheless, when the influence of ENSO is removed, in the tropical regions surrounding the Indian Ocean, there is a clear pattern of warm temperature anomalies over land regions to the west and cool anomalies over regions to the east of the Indian Ocean (Saji and Yamagata 2003). Over the extratropics, IOD is associated with warm temperature anomalies, reduced rainfall and positive geopotential height anomalies. The interannual variation of rainfall over central Brazil and subtropical La Plata Basin during austral spring is found to be influenced by the IOD, with a positive IOD associated with increased rainfall over the subtropical La Plata Basin, while it is associated with decreased rainfall over central Brazil (Chan *et al* 2008). Another impact of the IOD is on the ‘maha’ rainfall in Sri Lanka during September to December. Warm SST anomalies in the WEIO associated with the IOD event lead to enhanced convergence in the lower troposphere over the WEIO, which in fact, extends up to Sri Lanka (Lareef *et al* 2003). This leads to increased rainfall activity over Sri Lanka. In general, El Nino events also lead to increase in the ‘maha’ rainfall (Rasmusson and Carpenter 1983; Ropelewski and Halpert 1987). Thus, the influence of IOD and ENSO on the Sri Lankan rainfall is inter-linked. However, the influence of IOD is highly significant even when the ENSO influence is statistically removed (Lareef *et al* 2003). Some of the recent studies suggest that the evolution of the ENSO itself is influenced by the SST variations in the Indian Ocean (Yu *et al* 2002), in particular the IOD events (Behera and Yamagata 2003; Annamalai *et al* 2005). Thus, the influences of the IOD events are not restricted on the regional climate.

The mechanisms of the global teleconnections of the IOD events are yet to be understood clearly.

## 7. Concluding remarks

ENSO, which is the dominant signal of tropical interannual variability has significant influence on the Indian Ocean. Research in the last decade clearly demonstrates that the IOD is a major signal of interannual climate variations in the region. The question whether IOD is independent of ENSO or not has been debated long and it turns out that the Indian Ocean can breed and nurture its own IOD by coupled air-sea processes, without being forced externally by the Pacific Ocean. Both analysis of observations and model simulations converge to the fact that IOD can be generated either by ENSO or otherwise. There is a general consensus that the modification of Walker cell during ENSO is associated with subsidence over SETIO which suppresses convection and can trigger a positive feedback leading to the development of an IOD. Mechanism that causes IOD formation in the absence of ENSO is still unclear, although there are indications that anomalies in Hadley circulation holds the key. Observations suggest that subsurface temperature anomalies, accompanied by strong westward current anomalies appear about 3 months before the SSTA (Horii *et al* 2008; Nagura and McPhaden 2008). Whether the preconditioning of the ocean, with a lifted thermocline in the east, is a necessary condition is yet to be established. This aspect is of particular relevance to the recent intensification of IOD activity and monsoon-IOD feedback (Abram *et al* 2008).

Following the availability of high quality sea surface wind data, ocean models have been able

to reproduce the IOD events remarkably well (Murtugudde *et al* 2000; Vinayachandran *et al* 2007). Coupled-models, on the other hand, have several limitations. Simulation of the cold tongue in the Pacific and the shape of thermocline in the Indian Ocean are poor (Zhong *et al* 2005; Saji *et al* 2006). These two are important factors affecting the simulation of IOD and its dependence on ENSO need to be carefully evaluated and improved. As noted by Cai *et al* (2005), unrealistic interactions between Indian and Pacific Oceans can occur in coupled models, and this finding calls for careful evaluation of processes in coupled models.

The eastern pole of the IOD is quite robust in its location that is anchored by coastal upwelling to the west of Sumatra. Consequently, the focus of process studies has mostly concentrated in the east. The west, on the other hand, has been less organized with regard to SST anomalies. Interestingly, convection emanating from the western pole of IOD and its movement towards the west coast of India has been a striking feature during IOD events (Gadgil *et al* 2004). Further, convection over the eastern and western Indian Ocean during the monsoon behaves like a sea-saw; enhancement of one is associated with the suppression of the other. There is a need to understand the ocean-atmosphere coupling in this region, particularly during the summer monsoon and its probable role in taking IOD events to maturity through its control over atmospheric convection.

Impact of IOD on the climate of Asia, Africa and Australia is significant and, therefore, it is absolutely necessary that the scientific community be able to forecast its evolution well in advance. Considering that this is a fully coupled phenomenon, a coupled model is a basic requirement. The strong IOD event of 2006 (Vinayachandran *et al* 2007) was successfully predicted by a coupled model but it had limited success in forecasting the evolution of the weak IOD event of 2007 (Luo *et al* 2008). Extremes of the Indian summer monsoon are found to coincide with the positive and negative IOD (Gadgil *et al* 2003, 2004) and therefore urgent need for a forecast arises from the Indian subcontinent. Result of forecasting experiments (Luo *et al* 2008) are encouraging and the usefulness of such a system for Indian summer monsoon as well as other regions where IOD affects rainfall, is yet to be tested and put into practice.

### Acknowledgements

This study was funded by the Indian Ocean Modeling Program (INDOMOD), Indian National Centre for Ocean Information Services (INCOIS), Ministry of Earth Sciences, Government of India.

### References

- Abram N J, Gagan M K, McCulloch T M, Wahyoe J C and Hantoro S 2003 Coral reef death during the 1997 Indian Ocean dipole linked to Indonesian wildfires; *Science* **301** 952–955 doi:10.1126/science.1083841.
- Abram N J, Gagan M K, Cole J E, Hantoro W S and Mudelsee M 2008 Recent intensification of tropical climate variability in the Indian Ocean; *Nat. Geosci.* **1** 849–853 doi:10.1038/ngeo357.
- Ajayamohan R S and Rao S A 2008 Indian Ocean dipole modulates the number of extreme rainfall events over Indian in a warming environment; *J. Meteorol. Soc. Japan* **86** 245–252.
- Ajayamohan R S, Rao S A and Yamagata T 2008 Influence of Indian Ocean dipole on poleward propagation of boreal summer intraseasonal oscillations; *J. Climate* **21** 5437–5454.
- Ajayamohan R S, Rao S A, Luo J J and Yamagata T 2009 Influence of Indian Ocean dipole on boreal summer intraseasonal oscillations in a coupled general circulation model; *J. Geophys. Res.* **114** doi:10.1029/2008JD011096.
- Alexander M A, Blade I, Newman M, Lanzante J R, Lau N C and Scott J D 2002 The atmospheric bridge: The influence of ENSO teleconnections on air-sea interactions over the global oceans; *J. Climate* **15** 2205–2231.
- Allan R J, Chambers D, Drosdowsky W, Hendon H, Latif M, Nicholls N, Smith I, Stone R and Tourre Y 2001 Is there an Indian Ocean dipole independent of the El Niño-southern oscillations?; *CLIVAR Exchanges* **6** 4–8.
- Annamalai H, Murtugudde R, Potemra J, Xie S P, Liu P and Wang B 2003 Coupled dynamics over the Indian Ocean: Spring initiation of the zonal mode; *Deep Sea Res. Part II* **50** 2305–2330.
- Annamalai H and Murtugudde R 2004 Role of the Indian Ocean in regional climate variability; *Geophys. Monogr. Ser.* **147** 213–246.
- Annamalai H, Xie S P, McCreary J P and Murtugudde R 2005 Impact of Indian Ocean sea surface temperature on developing El Niño; *J. Climate* **18** 302–319.
- Ashok K, Guan Z and Yamagata T 2001 Impact of the Indian ocean dipole on the relationship between the Indian monsoon rainfall and ENSO; *Geophys. Res. Lett.* **28** 4459–4502.
- Ashok K, Guan Z and Yamagata T 2003 Impact of the Indian Ocean dipole on the Australian winter rainfall; *Geophys. Res. Lett.* **30** 1821 doi:10.1029/2003GL017926.
- Ashok K, Guan Z, Saji N H and Yamagata T 2004 Individual and combined influences of ENSO and the Indian Ocean dipole on the Indian summer monsoon; *J. Climate* **17** 3141–3155.
- Behera S K and Yamagata T 2003 Influence of the Indian Ocean dipole on the Southern Oscillation; *J. Meteor. Soc. Japan* **81** 169–177.
- Behera S K, Luo J J, Masson S, Yamagata T, Delecluse P, Gualdi S and Navarra A 2003 Impact of the Indian Ocean dipole on the east African short rains; *Clim. Exch.* **27** 43–45.
- Behera S K, Luo J J, Masson S, Delecluse P, Gualdi S, Navarra A and Yamagata T 2005 Paramount impact of the Indian Ocean dipole on the east African short rains: A CGCM study; *J. Climate* **18** 4514–4530.
- Behera S K, Luo J J, Masson S, Rao S A, Sakumo H and Yamagata T 2006 A CGCM study on the interaction between IOD and ENSO; *J. Climate* **19** 1608–1705.
- Bequerol-Bernal A, Latif M and Legutke M 2002 On dipole like variability of sea surface temperature in the tropical Indian Ocean; *J. Climate* **15** 1358–1368.

- Birkett C, Murtugudde R and Allan T 1999 Indian Ocean climate event brings floods to east Africa's lakes and the Sudd marsh; *Geophys. Res. Lett.* **26** 1031–1304.
- Black E, Slingo J and Sperber K R 2003 An observational study of the relationship between excessively strong short rains in coastal east Africa and Indian Ocean SST; *Mon. Weather Rev.* **131** 74–94.
- Cai W, Hendon H and Meyers G 2005 Indian Ocean dipole like variability in the CSIRO Mark 3 coupled climate model; *J. Climate* **18** 1449–1468.
- Carton J A, Chepurin G, Cao X and Giese B S 2000 A Simple Ocean Data Assimilation analysis of the global upper ocean 1950–95, Part 1: methodology; *J. Phys. Oceanogr.* **30** 294–309.
- Chan S C, Behera S K and Yamagata T 2008 Indian Ocean dipole influence on south American rainfall; *Geophys. Res. Lett.* **35** L14S12 doi:10.1029/2008GL034204.
- Chang P, Yamagata T, Schopf P, Behara S K, Carton J, Kessler W S, Meyers G, Qu T, Schott F, Shetye S R and Xie S P 2006 Climate fluctuations of tropical coupled system: The role of ocean dynamics; *J. Climate* **19** 5122–5174.
- Chen M, Xie P, Janowiak J E and Arkin P A 2002 Global land precipitation: A 50-yr monthly analysis based on gauge observations; *J. Climate* **3** 249–265.
- Clarke A J and Liu X 1993 Observations and dynamics of semiannual and annual sea levels near the eastern equatorial Indian Ocean boundary; *J. Phys. Oceanogr.* **23** 386–399.
- Conway D, Hanson C E, Doherty R and Persechino A 2006 GCM simulations of the Indian Ocean dipole influence on east African rainfall: Present and future; *Geophys. Res. Lett.* **34** L03705 doi:10.1029/2006GL027597.
- Elliott J R, Jewson S P and Sutton R T 2001 The impact of the 1997/98 El Niño event on the Atlantic Ocean; *J. Climate* **14** 1069–1077.
- Fischer A S, Terry P, Guilyardi E, Gualdi S and Delecluse P 2005 Two independent triggers for the Indian Ocean dipole/zonal mode in a coupled GCM; *J. Climate* **18** 3428–3449.
- Francis P A 2006 *Extremes of Indian summer monsoon rainfall and the equatorial Indian Ocean oscillation*; Ph D thesis, Indian Institute of Science Bangalore 91pp.
- Francis P A, Gadgil S and Vinayachandran P N 2007 Triggering of the positive Indian Ocean dipole events by severe cyclones over the Bay of Bengal; *Tellus A* **59** (4) 461–475 doi:10.1111/j.1600-0870.2007.00254.x.
- Gadgil S, Srinivasan J, Nanjundiah R S, Kumar K K, Munot A A and Kumar K R 2002 On forecasting the Indian summer monsoon: The intriguing season of 2002; *Curr. Sci.* **4** 394–403.
- Gadgil S, Vinayachandran P N and Francis P A 2003 Droughts of Indian summer monsoon: Role of clouds over the Indian Ocean; *Curr. Sci.* **85** 1713–1719.
- Gadgil S, Vinayachandran P N and Francis P A 2004 Extremes of the Indian summer monsoon rainfall, ENSO and the equatorial Indian Ocean oscillation; *Geophys. Res. Lett.* **31** L12213 doi:10.1029/2004GL019733.
- Gill A E 1980 *Atmosphere-ocean dynamics*; Academic Press, 662pp.
- Goddard L and Graham N E 1999 Simulation skills of the SST-forced global climate variability of the NCEP-MRF9 and the Scripps-MPI ECHAM3 model; *J. Climate* **13** 3657–3679.
- Gualdi S, Guilyardi E, Navarra A, Masina S and Delecluse P 2003 The interannual variability in the Indian Ocean as simulated by a CGCM; *Clim. Dyn.* **20** 567–582.
- Guan Z and Yamagata T 2003 The unusual summer of 1994 in east Asia: IOD teleconnections; *Geophys. Res. Lett.* **30** L01540 doi:10.1029/2002GL016831.
- Guan Z, Ashok K and Yamagata T 2003 Summertime response of the tropical atmosphere to the Indian Ocean sea surface temperature anomalies; *J. Meteorol. Soc. Japan* **81** 533–561.
- Halkides D J, Han W and Webster P J 2006 The effects of the seasonal cycle on the development and termination of the Indian Ocean zonal dipole mode; *J. Geophys. Res.* **111** doi:10.1029/2005JC003247.
- Han W, Shinoda T, Fu L-L and McCreary J P 2006 Impact of atmospheric intraseasonal oscillations on the Indian Ocean dipole during the 1990s; *J. Phys. Oceanogr.* **111** 679–690.
- Hastenrath S 2002 Dipoles, temperature gradients, and tropical climate anomalies; *Bull. Amer. Meteor. Soc.* **83** 735–740.
- Hastenrath S, Nicklis A and Greischar L 1993 Atmospheric-hydrospheric mechanisms of climate anomalies in the western equatorial Indian Ocean; *J. Geophys. Res.* **98** 20219–20235.
- Hendon H H 2003 Indonesian rainfall variability: Impacts of ENSO and local air-sea interaction; *J. Climate* **16** 1775–1790.
- Horii T, Hase H, Ueki I and Masumoto Y 2008 Oceanic precondition and evolution of the 2006 Indian Ocean dipole; *Geophys. Res. Lett.* **35** L03607 doi:10.1029/2007GL032464.
- Huang B and Kinter J L 2002 Interannual variability in the tropical Indian ocean; *J. Geophys. Res.* **107** doi: 10.1029/2001JC001278.
- Ihara C, Kushnir Y, Canea M A and Pena V H D L 2007 Indian summer monsoon rainfall and its link with ENSO and Indian Ocean climate indices; *Int. J. Climatol.* **27** 179–187.
- Iizuka S, Matsuura T and Yamagata T 2000 The Indian Ocean SST dipole simulated in a coupled general circulation model; *Geophys. Res. Lett.* **27** 3369–3372.
- Iskandar I, Rao S A and Tozuka T 2009 Chlorophyll-a bloom along the southern coasts of Java and Sumatra during 2006; *Int. J. Remote Sensing* **30** 663–671.
- Kajikawa Y, Yasunari T and Kawamura R 2001 The role of local Hadley circulation over the western Pacific on the zonally asymmetric anomalies over the Indian Ocean; *J. Meteorol. Soc. Japan* **81** 259–276.
- Kayanne H, Iijima H, Nakamura N, McClanahan T R, Behara S K and Yamagata T 2006 Indian Ocean dipole index recorded in Kenyan coral annual density bands; *Geophys. Res. Lett.* **33** L19709 doi:10.1029/2006GL027168.
- Kiladis G N and Diaz H F 1989 Global climatic anomalies associated with the southern oscillation; *J. Climate* **2** 1069–1090.
- Klein S A, Soden B J and Lau N C 1999 Remote sea surface temperature variations during ENSO: Evidence for a tropical atmospheric bridge; *J. Climate* **12** 917–932.
- Krishnamurthy V and Kirtman B P 2003 Variability of the Indian Ocean: Relation to monsoon and ENSO; *Quart. J. Roy. Met. Soc.* **129** 1623–1646.
- Kumar K K, Rajagopalan B and Cane M A 1999 On the weakening relationship between the Indian monsoon and ENSO; *Science* **284** 2156–2159.
- Lareef Z, Rao S A and Yamagata T 2003 Modulation of Sri Lankan maha rainfall by the Indian Ocean dipole; *Geophys. Res. Lett.* **30** L21063 doi:10.1029/2002GL015639.
- Latif M, Dommegård D, Dima M and Grotzner A 1999 The role of Indian Ocean sea surface temperature in forcing

- east African rainfall anomalies during December–January 1997/98; *J. Climate* **12** 3497–3504.
- Lau N C and Nath M J 2004 Coupled GCM simulation of atmosphere-ocean variability associated with zonally asymmetric SST changes in the tropical Indian Ocean; *J. Climate* **17** 245–265.
- Li T, Wang B, Chang C P and Zhang Y 2003 A theory for the Indian Ocean dipole-zonal mode; *J. Atmos. Sci.* **60** 2119–2135.
- Luo J J, Behera S K, Masumoto Y and Sakuma H 2008 Successful prediction of the consecutive IOD in 2006 and 2007; *Geophys. Res. Lett.* **35** L14S02 doi:10.1029/2007GL032793.
- Madden R A and Julian P R 1972 Description of global scale circulation cells in the tropics with a 40–50 day period; *J. Atmos. Sci.* **29** 1109–1123.
- Masson S, Boulanger J P, Menkes C, Delecluse P and Yamagata T 2004 Impact of salinity on the 1997 Indian Ocean dipole event in a numerical experiment; *J. Geophys. Res.* **109** C02002 doi:10.1029/2003JC001807.
- Masumoto Y and Meyers G 1998 Forced Rossby waves in the southern tropical Indian Ocean; *J. Geophys. Res.* **103** 27589–27602.
- Meyers G 1996 Variation of Indonesian throughflow and the El Niño southern oscillation; *J. Geophys. Res.* **101** 12255–12263.
- Meyers G, McIntosh P, Pigot L and Pook M 2007 The years of El Niño, La Niña and interactions with the tropical Indian Ocean; *J. Climate* **20** 2872–2880.
- Murtugudde R and Busalacchi A J 1998 Salinity effects in a tropical ocean model; *J. Geophys. Res.* **103** 3283–3300.
- Murtugudde R and Busalacchi A J 1999 Interannual variability of the dynamics and thermodynamics of the tropical Indian Ocean; *J. Climate* **12** 2301–2326.
- Murtugudde R, McCreary J P and Busalacchi A J 2000 Oceanic processes associated with anomalous events in Indian Ocean with relevance to 1997–98; *J. Geophys. Res.* **105** 3295–3306.
- Nagura M and McPhaden M J 2008 The dynamics of zonal current variations in the central equatorial Indian ocean; *Geophys. Res. Lett.* **35** L23603 doi:10.1029/2008GL03961.
- Nicholls N 1989 Sea surface temperatures and Australian winter rainfall; *J. Climate* **2** 965–973.
- Nicholls N 1995 All-India summer monsoon rainfall and sea surface temperatures around northern Australia and Indonesia; *Quart. J. Roy. Meteorol. Soc.* **8** 1463–1467.
- Nicholson S E and Kim J Y 1997 The relationship of the El Niño-Southern Oscillation to African rainfall; *Int. J. Climatol.* **17** 117–135.
- Pant G B and Parthasarathy B 1981 Some aspects of an association between the southern oscillation and Indian summer monsoon; *Arch. Meteorol. Geophys. Biokl.* **29** 245–251.
- Perigaud C, McCreary J P and Zhang K Q 2003 Impact of interannual rainfall anomalies on Indian Ocean salinity and temperature variability; *J. Geophys. Res.* **108** doi:10.1029/2002JC001699.
- Rao S A, Behera S K, Masumoto Y and Yamagata T 2002 Interannual subsurface variability in the tropical Indian Ocean with a special emphasis on the Indian Ocean dipole; *Deep Sea Res. Part II* **49** 1549–1572.
- Rao S A and Yamagata T 2004 Abrupt termination of Indian Ocean dipole events in response to intraseasonal disturbances; *Geophys. Res. Lett.* **31** L19306 doi:10.1029/2004GL020842.
- Rao S A and Behera S K 2005 Subsurface influence on SST in the tropical Indian Ocean: Structure and interannual variability; *Dynam. Atmos. Ocean* **39** 103–135.
- Rao S A, Luo J J, Behera S K and Yamagata T 2009 Generation and termination of Indian Ocean dipole events in 2003, 2006 and 2007; *Climate Dyn.* 10.1007/s00382-008-0498-z.
- Rasmusson E M and Carpenter T H 1982 Variations in tropical sea surface temperature and surface wind fields associated with the southern oscillation/El Niño; *Mon. Weather Rev.* **110** 354–384.
- Rasmusson E M and Carpenter T H 1983 The relationship between eastern equatorial Pacific sea surface temperatures and rainfall over India and Sri Lanka; *Mon. Weather Rev.* **111** 517–528.
- Reverdin G, Cadet D and Gutzler D 1986 Interannual displacements of convection and surface circulation over the equatorial Indian Ocean; *Quart. J. Roy. Meteorol. Soc.* **122** 43–67.
- Ropelewski C F and Halpert M S 1987 Global and regional scale precipitation patterns association with El Niño/southern oscillation; *Mon. Weather Rev.* **115** 1606–1626.
- Saha K 1970 Zonal anomaly of sea surface temperature in equatorial Indian Ocean and its possible effect upon monsoon circulation; *Tellus* **XXII(4)** 403–409.
- Saji N H and Yamagata T 2003 Possible impacts of Indian Ocean dipole mode events on global climate; *Clim. Res.* **25** 151–169.
- Saji N H, Goswami B N, Vinayachandran P N and Yamagata T 1999 A dipole mode in the tropical Indian Ocean; *Nature* **401** 360–363.
- Saji N H, Xie S P and Yamagata T 2006 Tropical Indian Ocean variability in the IPCC 20th-century climate simulations; *J. Climate* **19** 4397–4417.
- Sarma V V S S 2006 The influence of Indian Ocean dipole (IOD) on biogeochemistry of carbon in the Arabian Sea during 1997–98; *J. Earth Syst. Sci.* **115** 433–450.
- Schott F A and McCreary J P 2001 The monsoon circulation of the Indian Ocean; *Prog. Oceanogr.* **51** 1–123.
- Schott F A, Xie S P and McCreary J 2009 Indian Ocean circulation and climate variability; *Rev. Geophys.* **47** RG1002 doi:10.1029/2007RG000245.
- Shankar D, Vinayachandran P N and Unnikrishnan A S 2002 The monsoon currents in the north Indian Ocean; *Prog. Oceanogr.* **52(1)** 63–120.
- Shinoda T and Han W 2005 Influence of the Indian Ocean dipole on atmospheric subseasonal variability; *J. Climate* **18** 3891–3909.
- Sikka D R 1980 Some aspects of the large-scale fluctuations of summer monsoon rainfall over India in relation to fluctuations in the planetary and regional scale circulation parameters; *Proc. Indian Acad. Sci. (Earth Planet Sci.)* **89** 179–195.
- Sikka D R and Gadgil S 1980 On the maximum cloud zone and the ITCZ over Indian longitudes during the southwest monsoon; *Mon. Weather Rev.* **108** 1122–1135.
- Song Q, Vecchi G A and Rosati A J 2007 Indian Ocean variability in the GFDL coupled climate model; *J. Climate* **20** 2895–2916 doi:10.1175/JCL14159.1.
- Streten N A 1981 Southern Hemisphere sea surface temperature variability and apparent associations with Australian rainfall; *J. Geophys. Res.* **86** 896–909.
- Streten N A 1983 Extreme distributions of Australian annual rainfall in relation to sea surface temperature; *Int. J. Climatol.* **3** 143–153.
- Tozuka T, Luo J J, Masson S and Yamagata T 2008 Tropical Indian Ocean variability revealed by self-organizing maps; *Clim. Dyn.* **31** 333–343 doi:10.1007/s00382-007-0356-4.
- Ueda H and Matsumoto J 2001 A possible triggering process of east-west asymmetric anomalies over the Indian Ocean

- in relation to 1997/98 El Niño; *J. Meteorol. Soc. Japan* **7** 8803–8818.
- Ummenhofer C C, Gupta A S, Pook M J and England M H 2008 Anomalous rainfall over southwest western Australia forced by Indian Ocean sea surface temperatures; *J. Climate* **21** 5113–5134 doi:10.1175/2008JCLI2227.1.
- Ummenhofer C C, Gupta A S, England M H and Reason C J C 2009 Contributions of Indian Ocean sea surface temperatures to enhanced east African rainfall; *J. Climate* **22** 993–1013 doi:10.1175/2008JCLI2493.1.
- Venzke S, Latif M and Villwock A 2000 The coupled GCM ECHO-2. Part II: Indian Ocean response to ENSO; *J. Climate* **13** 1371–1383.
- Vinayachandran P N and Shetye S R 1991 The warm pool in the Indian Ocean; *Earth Planet Sci.* **100** 165–175.
- Vinayachandran P N, Saji N H and Yamagata T 1999 Response of the equatorial Indian Ocean to an anomalous wind event during 1994; *Geophys. Res. Lett.* **26** 1613–1615.
- Vinayachandran P N, Iizuka S and Yamagata T 2002 Indian Ocean dipole mode events in an ocean general circulation model; *Deep Sea Res. Part II* **49** 1573–1596.
- Vinayachandran P N and Mathew S 2003 Phytoplankton bloom in the Bay of Bengal during the northeast monsoon and its intensification by cyclones; *Geophys. Res. Lett.* **30** doi:10.1029/2002GL016717.
- Vinayachandran P N, Kurian J and Neema C P 2007 Indian Ocean response to anomalous conditions in 2006; *Geophys. Res. Lett.* **34** L15602 doi:10.1029/2007GL030194.
- Vinayachandran P N and Nanjundiah R S 2009 Indian Ocean sea surface salinity variations in a coupled model; *Climate Dyn.* doi:10.1007/s00382-008-0511-6.
- Webster P J, Moore A M, Loschnigg J P and Leben R R 1999 Coupled ocean-atmosphere dynamics in the Indian Ocean during 1997–98; *Nature* **401** 356–360 doi:10.1038/43848.
- Wiggert J D, Murtugudde R G and Christian J R 2006 Annual ecosystem variability in the tropical Indian Ocean: Results from a coupled bio-physical ocean general circulation model; *Deep Sea Res. II* **53** 644–676.
- Wiggert J D, Vialard J and Behrenfeld M J 2009 (in press) Basinwide modification of dynamical and biogeochemical processes by the positive phase of the Indian Ocean dipole during the SeaWiFS era; *Indian Ocean Biogeochem. Processes and Ecol. Variability* (eds) Wiggert J D, Hood R R, Naqvi S W A, Smith S L and Brink K H (Washington DC: American Geophysical Union).
- Wyrtki K 1973 An equatorial jet in the Indian Ocean; *Science* **181** 262–264.
- Xie S P, Annamalai H, Schott F A and McCreary J P 2002 Structure and mechanisms of south Indian Ocean Climate Variability; *J. Climate* **15** 867–878.
- Yamagata T, Mizuno K and Masumoto Y 1996 Seasonal variations in the equatorial Indian Ocean and their impact on the Lombok Throughflow; *J. Geophys. Res.* **101(C5)** 12465–12473.
- Yamagata T, Behara S K, Rao S A, Gaun Z, Ashok K and Saji N H 2002 The Indian Ocean dipole: A physical entity; *CLIVAR Exchanges* **24** 15–18, 20–22.
- Yamagata T, Saji N H and Behera S K 2003 Comments on Indian Ocean dipole; *Bull. Am. Meteorol. Soc.* **84** 1440–1442.
- Yamagata T, Behera S K, Luo J-J, Masson S, Jury M R and Rao S A 2004 Coupled ocean-atmosphere variability in the tropical Indian Ocean; *Geophysical Monograph Series* (eds) Wang C, Xie S P and Carton J A **147** 414 pp.
- Yasunari T 1980 A quasi-stationary appearance of 30–40 day period in the cloudiness fluctuations during the summer monsoon over India; *J. Meteorol. Soc. Japan* **58** 225–229.
- Yu J Y, Mechoso R, McWilliams J C and Arakawa A 2002 Impacts of Indian Ocean on ENSO cycles; *Geophys. Res. Lett.* **29** doi:10.1029/2001GL014098.
- Yu Z and McCreary J P 2004 Assessing precipitation products in the Indian Ocean using an ocean model; *J. Geophys. Res.* **109** doi:10.1029/2003JC00210.
- Zhong A, Hendon H H and Alves O 2005 Indian Ocean variability and its association with ENSO in a global coupled model; *J. Climate* **18** 3634–3649.